

Minimal phrase composition revealed by intracranial recordings

Authors:

Elliot Murphy^{1,2}, Oscar Woolnough^{1,2}, Patrick S. Rollo^{1,2}, Zachary Roccaforte¹, Katrien Segaert^{3,4}, Peter Hagoort^{4,5}, Nitin Tandon^{1,2,6,*}

1. Vivian L. Smith Department of Neurosurgery, McGovern Medical School, University of Texas Health Science Center at Houston, Houston, TX, USA
2. Texas Institute for Restorative Neurotechnologies, University of Texas Health Science Center at Houston, Houston, TX, USA
3. School of Psychology & Centre for Human Brain Health, University of Birmingham, Birmingham, UK
4. Max Planck Institute for Psycholinguistics, Nijmegen, The Netherlands
5. Donders Institute for Brain, Cognition and Behaviour, Nijmegen, The Netherlands
6. Memorial Hermann Hospital, Texas Medical Center, Houston, Texas, USA

*Corresponding author: Nitin Tandon (nitin.tandon@uth.tmc.edu)

Number of figures: 6 (+4 suppl.)

1 **Abstract**

2 The ability to comprehend phrases is an essential component of language. Here we evaluate
3 the neural processes that enable the transition from single word processing to a minimal
4 compositional scheme using intracranial recordings. 19 patients implanted with penetrating
5 depth or surface subdural intracranial electrodes heard auditory recordings of adjective-noun,
6 pseudoword-noun and adjective-pseudoword phrases and judged whether the phrase
7 matched a picture. Stimulus-dependent alterations in broadband gamma power activity (BGA),
8 low frequency power or phase consistency, and phase-locking values across the
9 compositional network were analyzed. The posterior superior temporal sulcus (pSTS) and
10 temporo-occipital junction (TOJ) revealed a fine-structured cortical mosaic, with closely
11 neighboring tissue displaying exclusive sensitivity to either lexicality or phrase structure, but
12 not both. During phrase composition, greater functional connectivity was seen between pSTS-
13 TOJ and both pars triangularis and temporal pole. These two regions also encode anticipation
14 of composition in broadband low frequencies. These results implicate pSTS-TOJ as a crucial
15 hub for the retrieval and computation of minimal phrases. Overall, this work reveals an
16 interface of sparsely interwoven coding for lower and higher level linguistic features, coupled
17 with large-scale network organization, with direct relevance to our understanding of cognitive
18 networks in the human brain.

19 **Keywords:** composition, electrocorticography, semantics, posterior temporal lobe,
20 anticipation, human, language

21 Introduction

22 How the brain integrates individual word meanings to comprehend the meaning of multi-word
23 utterances is an issue that has vexed the cognitive neuroscience of language for decades.
24 How the brain computes ‘complex meaning’ (Hagoort, 2020) from combinations of multiple
25 lexical items is still largely a mystery. This linguistic compositional process – the combination
26 of words into larger structures with new and complex meaning – is also referred to as “Merge”
27 (Chomsky, 1995; Chomsky et al., 2019) or “Unification” (Hagoort, 2013).

28 The simplest form of studying complex meaning is by using minimal phrases such as in the
29 *red-boat* paradigm, which focuses on simple combinations of two words (Bemis & Pykkänen,
30 2011, 2013a; Bozic et al., 2015; Brennan & Pykkänen, 2012; Flick et al., 2018; Flick &
31 Pykkänen, 2020; Pykkänen, 2020; Westerlund et al., 2015; Westerlund & Pykkänen, 2014),
32 avoiding a range of confounds associated with more complex linguistic stimuli (Berwick, &
33 Stabler, 2019). A “red boat” is interpreted as a boat which is red, and not a red object which
34 hosts boat-related properties, with phrases delivering novel syntactic and conceptual formats
35 (Leivada & Murphy, 2021; Murphy, 2015a; Pietroski, 2018). Experimental work using the *red-*
36 *boat* paradigm implicates the left anterior temporal lobe (ATL), specifically the temporal pole
37 (Antonucci et al., 2008; Bemis & Pykkänen, 2011; Lambon Ralph et al., 2012; Pobric et al.,
38 2010; Westerlund & Pykkänen, 2014; Wilson et al., 2014; Zhang & Pykkänen, 2018), and
39 posterior temporal regions (Flick & Pykkänen, 2020; Matchin & Hickok, 2020) as crucial nodes
40 for phrase composition. *Red-boat* experiments isolate semantic composition, which in turn
41 encompasses syntactic composition. These studies report responses that vary in timing
42 (between 180–350ms post-composition) and duration (50–100ms). The left posterior temporal
43 lobe and angular gyrus (AG) also show greater activity for sentences than word lists, and for
44 phrases than words (Brennan et al., 2016; Matchin & Hickok, 2020), making them candidate
45 regions for the retrieval of phrasal templates (Hagoort, 2003, 2017),

46 Phrase composition is a rapid process that is likely dependent on finely organized sets of
47 distributed cortical substrates. Previous work in the *red-boat* paradigm has been limited by
48 spatiotemporal resolution. Using recordings from intracranial electroencephalography (iEEG)
49 with depth electrodes penetrating grey matter or electrodes located on the cortical surface, we
50 conducted a study of minimal phrase composition with auditory presentations of adjective-
51 noun phrases across a large patient cohort (n = 19).

52 We utilized grammatical noun phrases (“red boat”) and pseudoword phrases with variable
53 positions of the pseudoword (“bleeg boat”, “red fulg”) to isolate semantic compositional
54 processing. An adjective-pseudoword condition (“red fulg”) was included to isolate semantic
55 compositionality and reduce predictability. Given the large number of patients in our study, we

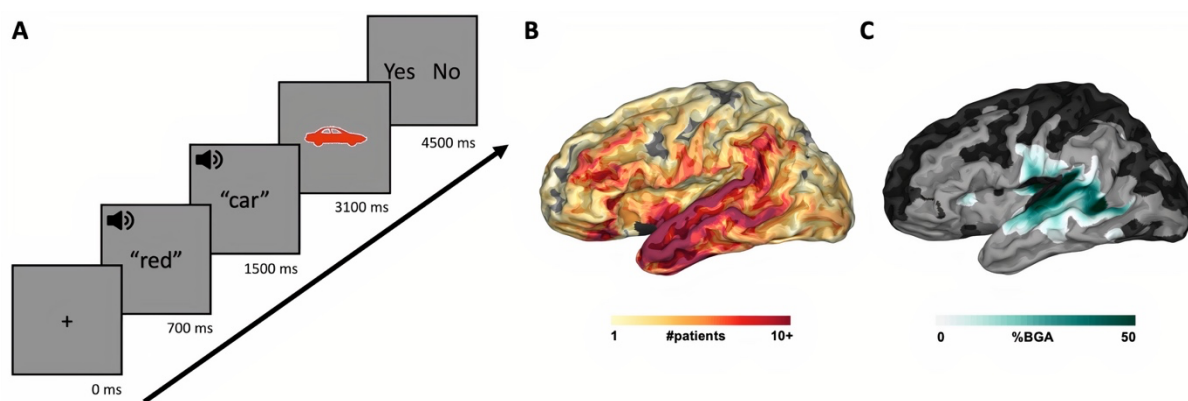
56 were able to analyze not only regions of interest delineated by previous studies, but also a
57 range of temporal, frontal and parietal cortices not previously implicated in models of phrase
58 composition.

59 Studies using scalp electroencephalography and magnetoencephalography (MEG) were used
60 to constrain our analytic space. iEEG provides uniquely high spatiotemporal resolution
61 recordings and is less susceptible to artifacts (e.g., muscle movements) (Arya, 2019; Flinker
62 et al., 2011). High frequency gamma changes (Conner et al., 2019; Forseth et al., 2018;
63 Johnson et al., 2020; Leszczyński et al., 2020; Towle et al., 2008; Yi et al., 2019) typically
64 index local cortical processing and are implicated in a range of cognitive processes (Buzsáki
65 & Watson, 2012; Hovsepyan et al., 2020; Jensen et al., 2019; Marko et al., 2019; Packard et
66 al., 2020; Prystauka & Lewis, 2019). An early anterior negative deflection immediately
67 preceding the critical noun in combinatorial contexts (-50–100ms) (Neufeld et al., 2016) likely
68 indexes syntactic prediction (Lau et al., 2006). Low frequency power increases have also been
69 noted during the anticipatory window (Bastiaansen & Hagoort, 2015; Lewis et al., 2016;
70 Segaert et al., 2018), during phrase composition (Segaert et al., 2018) and in a variety of
71 auditory phrase and sentence processing paradigms (Ding et al., 2016; Keitel et al., 2018;
72 Keitel et al., 2017; Mai et al., 2016). Therefore, we also evaluated the role of low frequencies
73 during anticipatory composition. Lastly, our task required patients to determine whether the
74 words they heard matched a subsequent image, enabling analyses related to phrase-matched
75 and phrase-contrasted contexts.

76

77 **Results**

78 Patients were presented with auditory recordings grouped randomly into three conditions:
79 Adjective-Noun, Pseudoword-Noun, Adjective-Pseudoword. A subsequent colored image was
80 presented, and patients were tasked with responding, with a button press, to whether the
81 image matched the phrase or not (Fig. 1A). Across the cohort, we had good coverage over
82 lateral and medial temporal lobe, inferior parietal lobe and inferior frontal regions, with some
83 coverage reaching into other portions of fronto-parietal regions (Fig. 1B). We saw activation
84 in response to the auditory stimuli most prominently in superior and middle temporal regions
85 (Fig. 1C). Below we report results pertaining to lexicality; phrase anticipation; phrase
86 composition; and linguistic-visual unification.



87

88 **Figure 1: Experimental paradigm with coverage and activation maps.** (A) Experimental
89 design. Average stimuli length: adjectives (420 ± 39 ms; mean \pm SD), nouns (450 ± 75 ms),
90 pseudowords (430 ± 38 ms). (B) Group coverage map of included, left hemisphere electrodes,
91 plotted on a semi-inflated standardised N27 surface. (C) Broadband gamma activity (BGA)
92 increases from baseline (-500 to -100ms prior to first word) for all conditions from 100 to 400ms
93 after onset of the first word (threshold: %BGA > 5%, $t > 1.96$, patient coverage ≥ 3 ; $p < 0.01$
94 corrected). Black surfaces fell below patient coverage threshold.

95

96 Behavioral performance

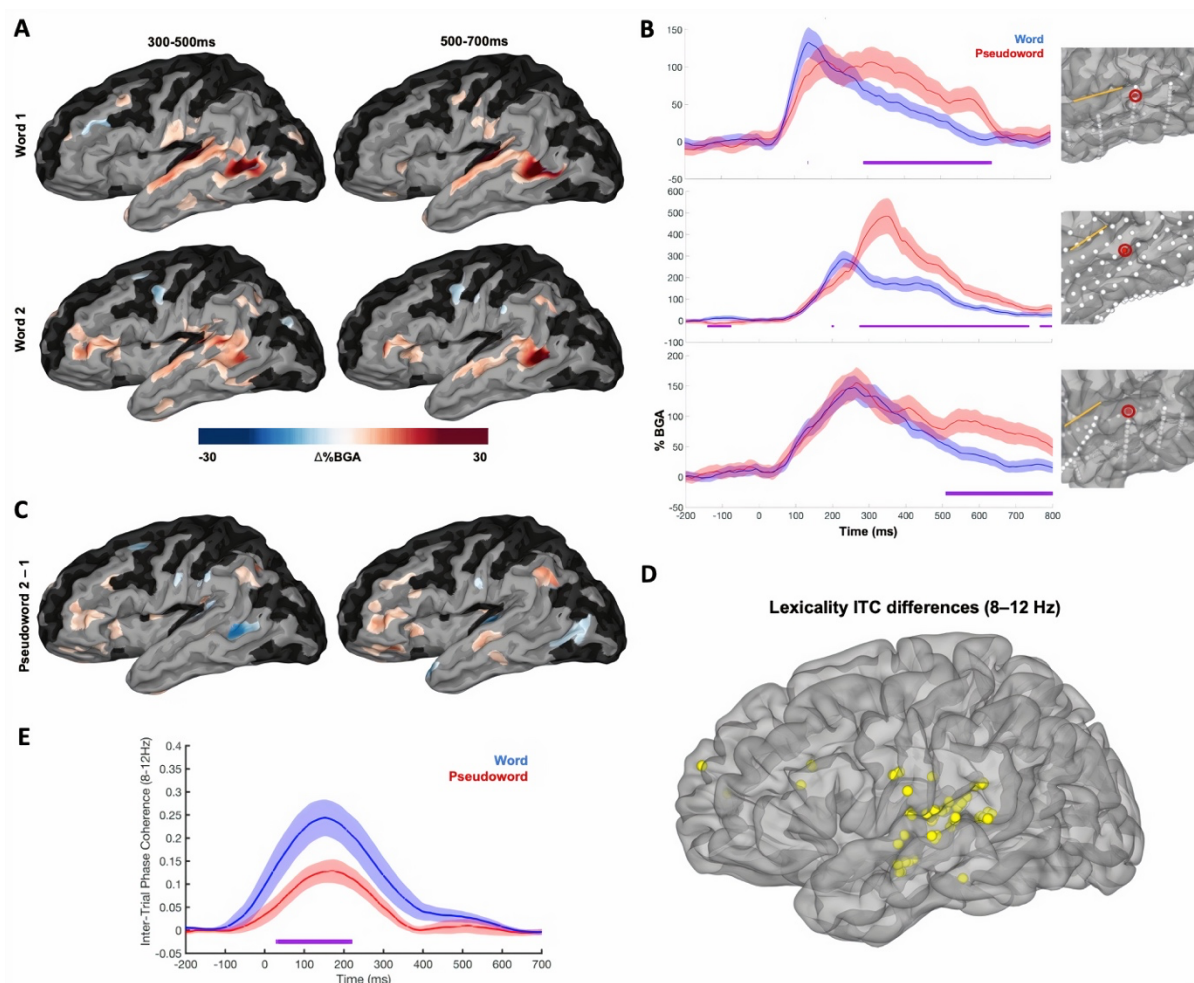
97 Performance in the image matching task was highly accurate $97 \pm 3\%$ ($311 \pm 11/320$ trials)
98 with an average response time of 1599 ± 539 ms. Only correct trials were analyzed further.

99

100 Effects of lexicality

101 To disentangle single word semantic effects from those of combinatorial semantics, we probed
102 the difference in representation of words vs. pseudowords. We generated a surface-based,
103 population-level map of cortical activity using a surface-based mixed-effects multi-level
104 analysis (SB-MEMA) (Conner et al., 2011; Fischl et al., 1999; Kadipasaoglu et al., 2014;
105 Kadipasaoglu et al., 2015), a method specifically designed to account for sampling variations
106 in iEEG and minimize effects of outliers. An SB-MEMA contrasting adjectives vs. pseudowords
107 in word position 1 and nouns vs. pseudowords in word position 2 (Fig. 2A) revealed
108 significantly greater broadband gamma activity (BGA; 70–150 Hz) for pseudowords than
109 words in posterior superior temporal gyrus (pSTG), posterior superior temporal sulcus (pSTS),
110 temporo-occipital junction (TOJ) and pars triangularis 300–700ms after word onset, indexing
111 the additional processing of unfamiliar word sounds in an attempt to derive potential lexicality.
112 The greater BGA increase for pseudowords than words at position 2 than position 1 around

113 pars triangularis and surrounding frontal areas (Fig. 2C), suggests involvement of this region
 114 in effortful lexical processing (perhaps in phonological space) to facilitate semantic unification
 115 (Hagoort, 2005, 2013; Hagoort & Indefrey, 2014).



116
 117 **Figure 2: Grouped analysis for lexicity.** (A) SB-MEMA comparing words vs pseudowords,
 118 red colors indexes greater BGA (70–150 Hz) for pseudowords and blue colors for words
 119 (threshold: %BGA > 5%, $t > 1.96$, patient coverage ≥ 3 ; $p < 0.01$ corrected). Top row: word
 120 position 1; bottom row: word position 2. (B) Exemplar electrodes for the words vs pseudowords
 121 analysis (red: pseudowords; blue: words). Error bars (colored shading) set at one standard
 122 error. Sylvian fissure is marked with a yellow line for reference on each surface. (C) SB-MEMA
 123 indicating BGA increases for pseudowords at the second word position relative to
 124 pseudowords at the first word position. (D) Electrodes with significant differences in inter-trial
 125 phase coherence (ITC) for words vs pseudowords, in posterior temporal cortex (9 patients).
 126 (E) ITC in alpha (8–12 Hz) at all electrodes in (D) for words (blue) and pseudowords (red) on
 127 the left. T0 = first word onset.

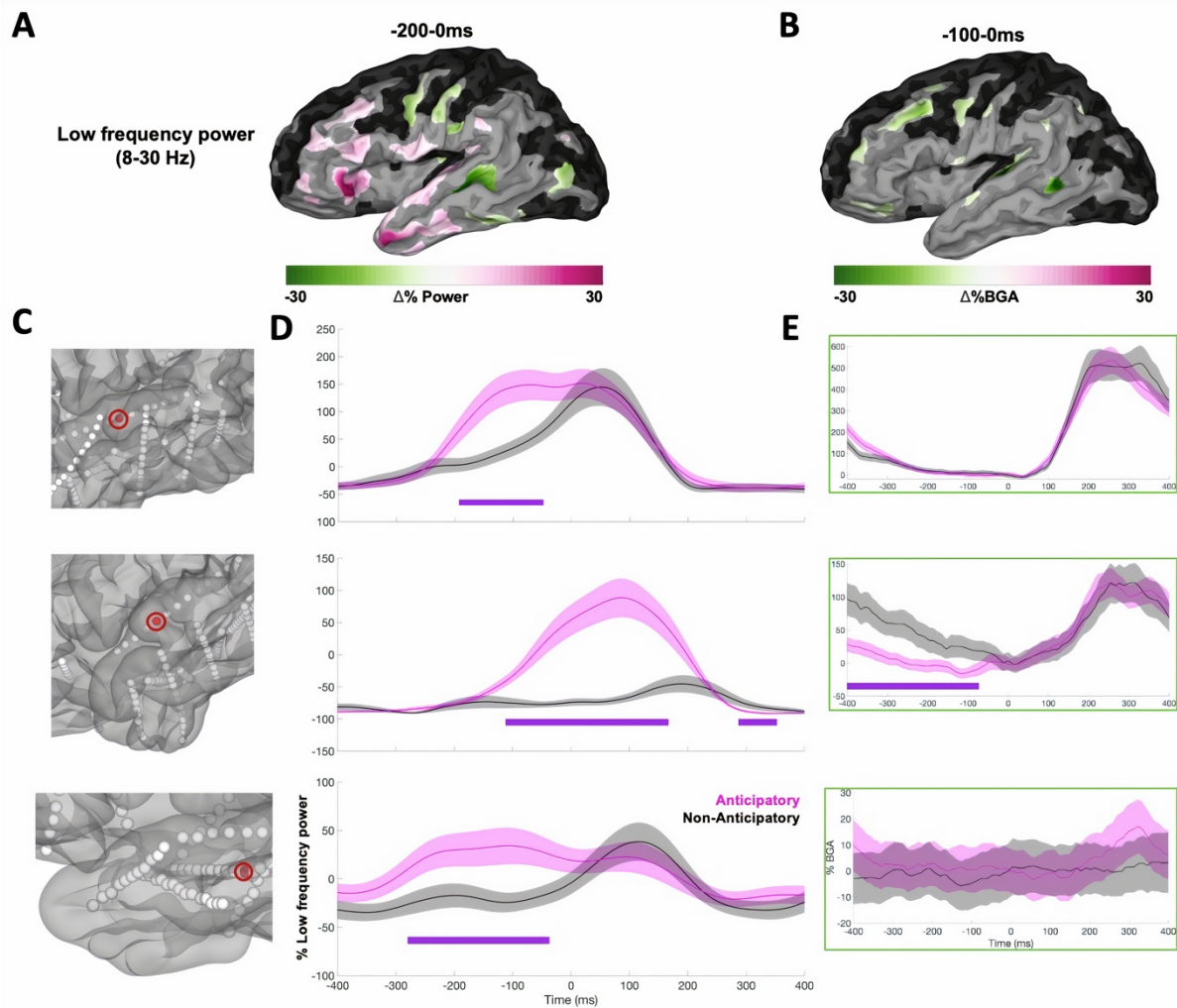
128

129 Additionally, to broaden our assessment of the contributions of lower frequencies, we
130 computed inter-trial phase coherence (ITC) across regions and low frequencies. We found
131 significantly greater ITC values for words relative to pseudowords in and around pSTG (Fig.
132 2D, E; Suppl. Fig. 1) in the alpha band (8–12 Hz). No other ROIs (ATL, pars triangularis, pars
133 orbitalis, MTG, supramarginal gyrus: all FDR-corrected q-values >0.05) displayed such effects
134 for this, or for phrase composition. Alpha phase coherence in pSTG may therefore encode
135 information relevant to lexical interpretation.

136

137 Compositional anticipation

138 We next contrasted Adjective-Noun and Pseudoword-Noun conditions at the onset of second
139 word presentation, with only the former condition licensing any phrasal anticipation. During
140 the anticipatory window for phrase formation (from -200ms to 0ms prior to the second word
141 onset), low frequency power (8–30 Hz) exhibited an anticipatory effect (Fig. 3). This
142 anticipatory effect was found in IFG, pSTG and ATL, which all appear to be involved in
143 syntactic-semantic prediction generation. In addition, these anticipatory effects were unrelated
144 to BGA, and such widespread, regional effects were not found in delta or theta. For
145 comparison, we also plot the anticipatory window in BGA for -100 to 0ms (Fig. 3B), which
146 exhibited no relation with the lower frequency effects (compare also Fig. 3D with Fig. 3E).



147

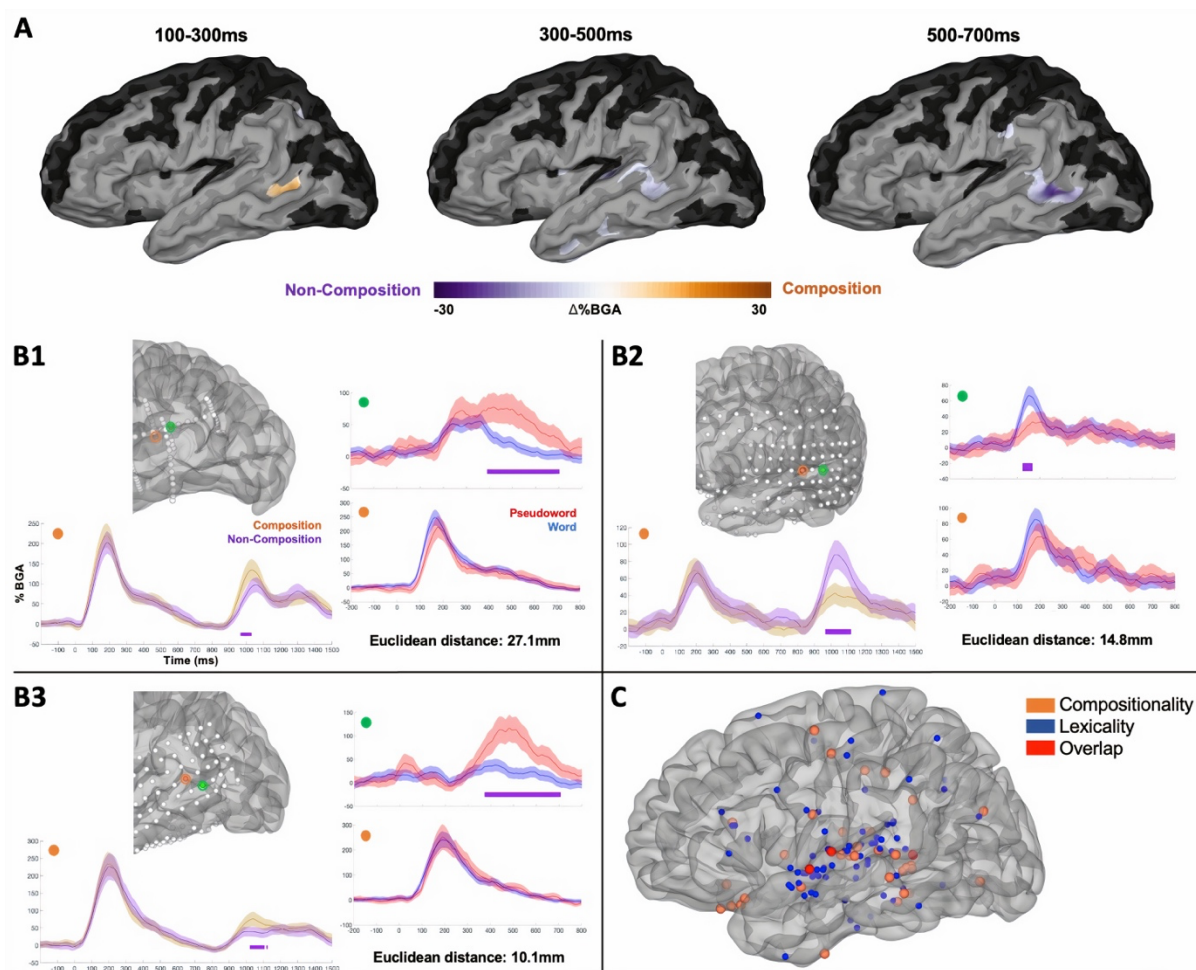
148 **Figure 3: Syntactic-semantic compositional anticipation.** (A) SB-MEMA for the
 149 anticipatory time window centred around second word onset (-200–0ms) for low frequency
 150 power. Pink: Greater power for composition anticipation. Green: Greater for no anticipation
 151 (i.e. after having heard a Pseudoword at first word position). (B) SB-MEMA for BGA for the
 152 same contrast for -100–0ms prior to second word onset. (C)-(E) Exemplar electrodes with
 153 location (C), low frequency power traces and (D) BGA traces in dashed green boxes (E),
 154 across three patients sorted by row.

155

156 Phrase composition

157 The full combinatorial contrast (Adjective-Noun vs [Adjective-Pseudoword + Pseudoword-
 158 Noun]), revealed greater BGA for portions of pSTS-TOJ during phrase composition than non-
 159 composition (Fig. 4A). The specific onset of this effect was around 210ms after noun onset,
 160 with peak BGA at around 300ms (Suppl. Fig. 3). The same region exhibited greater BGA for
 161 non-composition at later time points, implicating it in effortful phrase structure derivations.

162 Certain portions of pSTS-TOJ across patients displayed exclusive sensitivity to phrase
 163 composition, and not lexicality (Fig. 4B). Other regions – pSTG and inferior frontal gyrus (IFG)
 164 – did not show any significant BGA differences between these conditions (Suppl. Fig. 2). Since
 165 previous combinatorial effects in phrasal and sentential processing have also localized to
 166 anterior temporal pole, we also focused on this region (Suppl. Fig. 2, 4). These portions of left
 167 anterior temporal lobe (temporal pole) exhibited increased broadband low frequency activity
 168 in response to phrases from approximately 380–460ms and 700–900ms after noun
 169 presentation. This activity was unrelated to BGA, indicating that low frequency activity in ATL
 170 is an independent component of phrase structure comprehension; likely late-stage semantic
 171 processing. The ERPs were dissociable from BGA across the ROIs plotted (Suppl. Fig. 2): A
 172 late effect for Non-Composition was found in Broca’s area, likely due to greater attempted
 173 lexical access for the pseudowords, while a late signature was detected in temporal pole for
 174 Composition, potentially related to late-stage conceptual access.



175

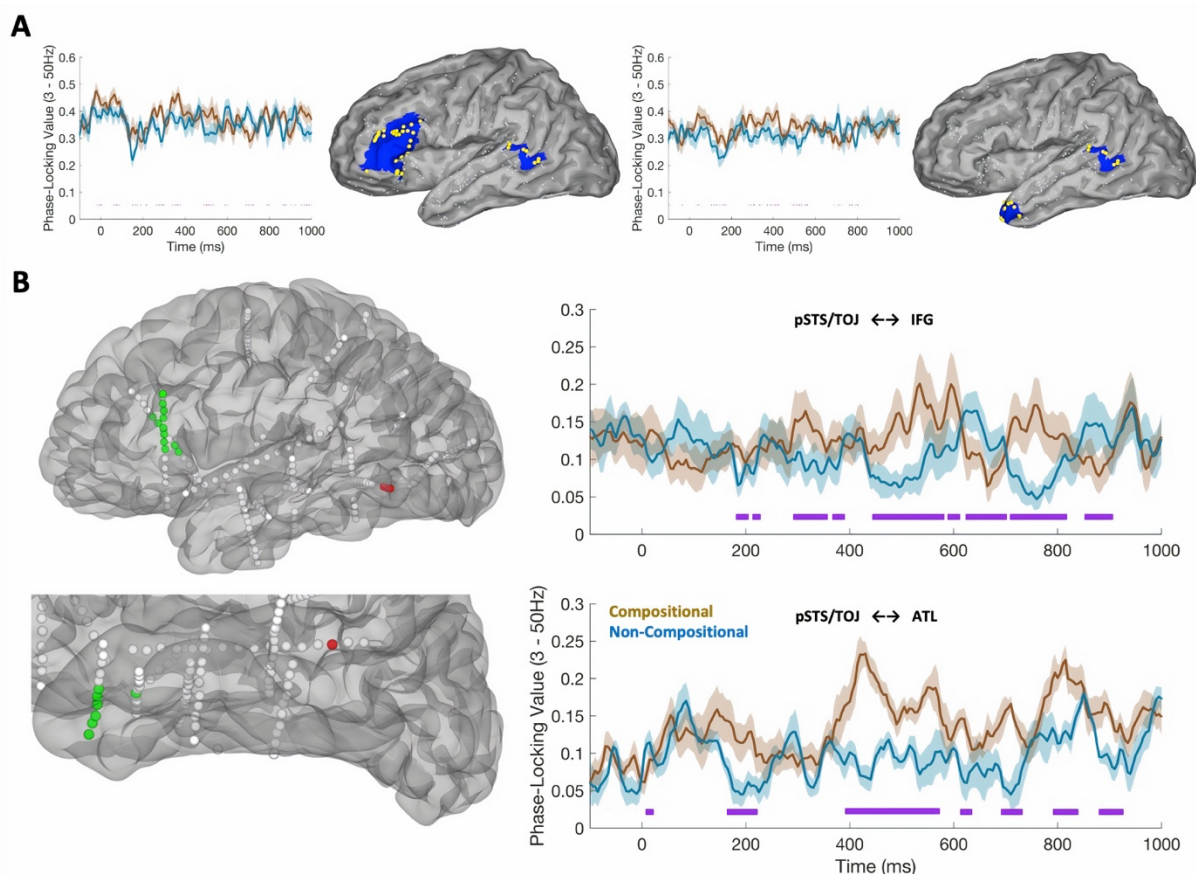
176 **Figure 4: Grouped analysis for phrase composition.** (A) SB-MEMAs for the phrase
 177 composition analysis for BGA. (B) Exemplar electrodes with FDR-corrected (one-tailed t-tests,
 178 $q < 0.05$) significance bars in purple plotted in native patient space. Includes compositional

179 contrast and lexicality contrast, dissociating neighbouring portions of pSTS-TOJ that
180 responded exclusively for phrase composition and not lexicality (orange dots = composition
181 effect; green dots = lexicality effect). Error bars set at one standard error. Numbers denote
182 distinct patients. (C) Electrodes exhibiting a significant BGA contrast between Compositional
183 and Non-Compositional trials. 39 electrodes (orange) from 12 patients exhibited an FDR-
184 significant contrast (one-tailed t-tests, $q < 0.05$) for compositionality at some point between 0-
185 1000ms after the second word; 97 electrodes across 17 patients for lexicality; 3 electrodes for
186 both across 3 patients.

187

188 Next, we isolated regions of interest to derive cortical functional connectivity during phrase
189 composition. These were based either on results from our main analysis (pSTS-TOJ, temporal
190 pole) or on composition effects described in the literature (inferior frontal regions). To
191 characterize functional connectivity between these regions during phrase composition, we
192 computed phase-locking values (PLV) for electrode pairs situated within pSTS-TOJ with either
193 pars triangularis or anterior temporal lobe. We computed the generalized phase of the
194 wideband filtered (3–50 Hz) signal that has previously been shown to be more effective than
195 the use of narrowband alpha or theta filters (Davis et al., 2020).

196 Among patients with concurrent coverage in pSTS-TOJ and pars triangularis ($n = 8$, electrode
197 pairs = 231), the majority ($n = 5$) exhibited significantly greater PLVs for Compositional than
198 for Non-Compositional trials during the 0–500ms period after second word onset, averaging
199 across PLV values for each pair. In patients with joint coverage in pSTS-TOJ and anterior
200 temporal lobe (temporal pole) ($n = 8$, electrode pairs = 274), the majority ($n = 6$) showed
201 greater PLVs for the same contrast during the same time window. We plot the magnitude of
202 phase-locking values across these regions and in two exemplar patients (Fig. 5).



203

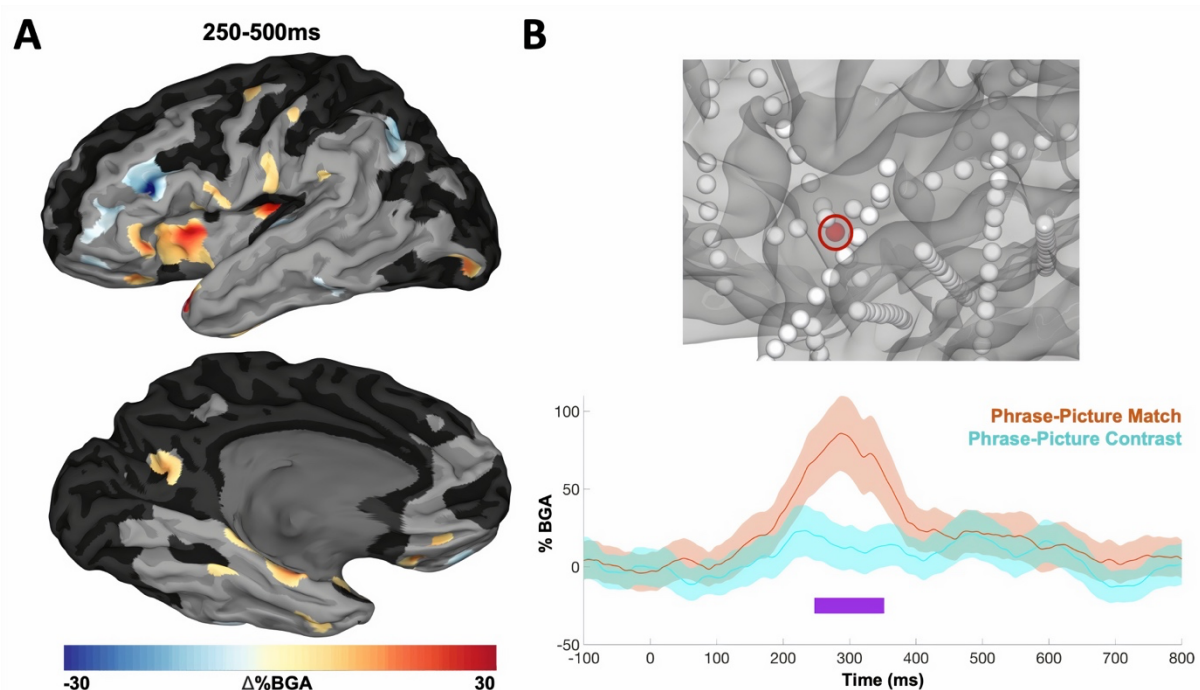
204 **Figure 5:** Phase-locking between semantic composition regions of interest. (A) Left: Average
 205 generalized phase-locking values (gPLV) for 5 patients showing greater gPLV for phrase
 206 composition relative to non-composition between pSTS-TOJ (HCP index: TPOJ1) and pars
 207 triangularis (HCP index: 45, IFSa, IFSp, 47I). Right: The same plot but for the 6 patients
 208 showing greater gPLV between pSTS-TOJ and temporal pole (HCP index: TGd). (B) Posterior
 209 temporal lobe (pSTS-TOJ) gPLVs with inferior frontal gyrus (specifically, pars triangularis)
 210 (Top) and anterior temporal lobe (specifically, temporal pole) (Bottom). Left plots show the
 211 localization in native space of electrodes significantly involved ($q < 0.05$) in inter-regional
 212 phase-locking (3–50 Hz). Right plots show average time courses (mean \pm SEM) of phase-
 213 locking value changes from baseline in phrase composition (brown) and non-composition
 214 (blue) trials.

215

216 Integration of linguistic and visual information

217 Following each phrase, patients were presented with a matching or non-matching visual
 218 representation of the phrase. Comparing the Adjective-Noun trials which contained a matching
 219 picture, or a non-matching picture, during the 250–500ms post-picture window, SB-MEMAs
 220 revealed two notable effects (Fig. 6): Anterior insula exhibited greater BGA for phrase-picture

221 matches, while more dorsal frontal regions, centered around inferior frontal sulcus, exhibited
222 greater BGA for phrase-picture non-matches. Thus, these regions appear to be implicated in
223 linguistic-visual integration and monitoring, likely anchored around the semantic content
224 denoted by both phrases and images and their successful association via some conjunction
225 operator (i.e. [*red* \wedge *boat*], rather than a monadic adjectival or nominal representation). These
226 two regions flank Broca's area, subserving distinct composition-related goals. Since activity of
227 opercular regions can be misattributed to the insula (Woolnough et al., 2019), we ensured that
228 these effects across patients specifically came from electrodes in insula proper, rather than
229 operculum or Broca's area.



230

231 **Figure 6: Grouped analysis for linguistic-visual integration.** (A) SB-MEMA in BGA for
232 phrase-picture match (orange) and phrase-picture contrast (turquoise) increases, 250–500ms
233 after picture onset. (B) Exemplar insula electrode.

234

235 Discussion

236 We localized the neural signatures of combinatorial phrase structure comprehension using
237 minimal adjective-noun phrases in a large patient cohort, with both penetrating depth and
238 surface grid intracranial electrodes. We identified a broad portion of posterior temporal cortex
239 as being sensitive to lexicality, and then isolated closely neighboring portions of pSTS-TOJ
240 within patients that responded exclusively to phrase composition, and not lexicality, and vice
241 versa. This computational contrast within a narrow strip of pSTS-TOJ provides a finely

242 organized cortical mosaic for the language system (Amunts & Zilles, 2015), going beyond
243 more traditional, broader structure-function mappings for higher-order syntax-semantics. Our
244 results can contribute to the development of a micro-map of pSTS-TOJ with respect to the
245 demands of computational complexity; a necessary step towards understanding the
246 organizational principles of the brain at distinct spatial scales, including ultimately cellular
247 components.

248 Phrase composition was indexed by two main components: Greater BGA in portions of pSTS-
249 TOJ at an early window (around 210-300ms); greater low frequency power in temporal pole
250 at 380–460ms and 700–900ms after the presentation of a phrase-licensing nominal. Greater
251 functional connectivity for phrase composition was found between these regions (pSTS-TOJ
252 and temporal pole) and also between pSTS-TOJ and pars triangularis. pSTS-TOJ is initially
253 active for phrase composition and subsequently shows greater local cortical activity for non-
254 compositional stimuli, indicating its involvement in phrase-related processing. In addition,
255 pSTS-TOJ and pSTG encode local processing of pseudowords, with pSTG likely coding
256 speech signals into articulatory representations (Martin et al., 2019). Anterior portions of IFG
257 exhibit greater BGA for pseudowords at the second word position, possibly indexing increased
258 unification demands with the preceding adjective, compared to a real word (Hagoort, 2005,
259 2013; Hagoort & Indefrey, 2014). This effect may hence index the role of this region in the
260 syntactic and semantic unification of more or less expected continuations, in agreement with
261 earlier results in a sentence context (Hagoort, 2004).

262 In addition, STG, ATL and IFG index composition anticipation in low frequency power,
263 consistent with a predictive neural mechanism for higher-order linguistic information
264 (Bastiaansen & Hagoort, 2015; Benítez-Burraco & Murphy, 2019; Lewis et al., 2016; Murphy,
265 2015b; Prystauka & Lewis, 2019). These anticipatory effects were found in the context of our
266 stimuli being controlled for predictability (the addition of the Adjective-Pseudoword condition is
267 the simplest way to achieve this). We additionally showed that alpha phase encodes lexical
268 information exclusively in pSTG via ITC (and not phrase-relevant information).

269 Lastly, anterior insula and inferior frontal sulcus (IFS) subserve the integration of language
270 input with the visual referent. Both of these regions have been argued to be the convergence
271 zones of the ventral (anterior insula) and dorsal (IFS) attentional networks (Cazzoli et al.,
272 2021), while task-evoked pupillary dynamics have been linked to the insula (Kucyi & Parvizi,
273 2020); given current task demands, these dynamics may also underscore our findings.

274 Lexicality

275 Our results replicate prior studies in which BGA localized to p/mSTG and pSTS tracks lexicality
276 (Canolty et al., 2007; Humphries et al., 2006; Tanji et al., 2005). In addition, we show

277 recruitment of anterior IFG in this process. Further, pSTG alpha phase coherence may index
278 the coordination of smaller-scale ensembles which may bundle sub-lexical features to yield
279 coherent word-level interpretations of auditory stimuli, in accord with a recent
280 neurocomputational model for lexical feature-set construction (Murphy, 2020).

281 Anticipatory response

282 According to a range of parsing models (Berwick et al., 2019), adjective-noun syntax is
283 constructed predictively, in anticipation of the noun. Neural response differences in the period
284 preceding the noun in combinatorial trials would likely reflect the generation of this structure.
285 For instance, particular anticipatory amplitude increases have been isolated to the alpha (8–
286 12 Hz) and beta (15–30 Hz) bands in fronto-central and fronto-temporal scalp EEG electrodes,
287 and have been related to the pre-activation of linguistic structure/information (Gastaldon et al.,
288 2020; Segaert et al., 2018). Based on our results, low frequency power in IFG and ATL may
289 be preparing a syntactic slot to be filled by predicted upcoming nominal content, or initiating
290 top-down local coordination of subsequent composition-indexing BGA in pSTS-TOJ. These
291 low frequency dynamics might not even pertain to lexico-semantic prediction specifically, but
292 rather anticipatory stages pertaining to phrasal initiation (Terporten et al., 2019). Our findings
293 are also potentially in line with the notion that beta oscillations can index the construction and
294 maintenance of sentence-level meaning (scaling up from minimal phrases) (Lewis et al.,
295 2016), and the claims that beta can index aspects of syntactic anticipation and phrasal
296 category generation (Benítez-Burraco & Murphy, 2019; Murphy, 2020).

297 Our results may relate to increased recruitment (Bonnefond & Jensen, 2013) of pSTS in late
298 stage lexical processing effort (-200–0ms before the noun). The portion of temporal pole and
299 MTG exhibiting low frequency increases during the anticipatory window could be also involved
300 in late-stage lexico-conceptual processing of adjectival representations, although given the
301 relatively late post-adjective window it is more likely to be related to anticipation. Given
302 increasing evidence for IFG involvement in linear morpho-syntactic processing (Matchin &
303 Hickok, 2020), it is also possible that effects in IFG index a form of lexical anticipation.
304 Predictable word processing specifically pinpoints anterior IFG and ATL in preceding cortical
305 activations (Pulvermüller & Grisoni, 2020). During basic semantic composition, anterior IFG
306 activation has been shown to increase with the amount of lexical information being integrated
307 into the structure (Schell et al., 2017), again pointing to a role for this region as a lexical
308 memory buffer and/or the locus of higher-order predictions.

309 Minimal phrase composition

310 We found that neighbouring portions of pSTS-TOJ across patients can exclusively code either
311 for lexicality or phrase composition, helping to isolate the core compositional operation in

312 phrase structure generation. While a large area of posterior and superior temporal cortex was
313 sensitive to lexicality, a narrower portion was recruited exclusively to code for phrase structure,
314 generating from simple lexical meanings the more computationally demanding structures of
315 'complex meaning' (Hagoort, 2020; Pietroski, 2018).

316 One of the main candidates for phrase composition from previous research, ATL, was
317 implicated via low frequency activity (specifically, temporal pole activity). This may indicate
318 that temporal pole is involved in compositional processing within a noun phrase, with low
319 frequency activity possibly coordinating broader areas in the service of constructing a coherent
320 semantic referent (Wang et al., 2020). Despite ATL being the "most consistent integrative
321 node" (Pylkkänen & Brennan, 2020) in the syntax-semantics combinatorial network, the high
322 spatiotemporal resolution of iEEG presented another candidate for composition: pSTS-TOJ.
323 Increasing morpho-orthographic complexity in a similar minimal phrasal paradigm does not
324 implicate ATL in early processing windows, but seems to delay ATL activity until after intra-
325 word morphological composition (Flick et al., 2018). This suggests that there must be regions
326 independent of semantic and orthographic processing that are common to all forms of (early)
327 phrasal composition. Our findings suggest that pSTS-TOJ might be one such region, although
328 since we only presented auditory stimuli we cannot make any stronger claims. Comparing the
329 discovered composition effect in BGA (Fig. 4A) with the auditory stimuli activation map (Fig.
330 1C) suggests a clear overlap between sites of initial sensitivity to auditory stimuli and
331 composition-sensitive sites. On the other hand, while there is indeed overlap, there is also a
332 portion of posterior TOJ which seems uniquely active for composition but which is not
333 prominently sensitive to audition, which may point to the involvement of a more modality-
334 independent compositional process. Since MEG cannot detect high frequency activity deep in
335 sulci (Irimia et al., 2012), our iEEG investigation was able to provide new insights here.

336 With respect to activation timings, we found greater BGA for phrase composition in pSTS-TOJ
337 at 210ms, diminishing around 300ms, after which the majority of responses were greater for
338 non-compositional trials. It is possible that composition-specific computations initiated earlier
339 than this, and that it was only during these time windows that condition differences arose. The
340 later, greater responses for non-composition could be due to more efficient encoding of
341 phrases (hence lower BGA), or, more likely given the latency, late-stage compositional
342 effort/evaluation. It is also possible that the low frequency responses we found to composition
343 in ATL are responses to post-syntactic (pSTS-TOJ) processing, leading to conceptual
344 integration. The timing of these late wrap-up effects might be due to the slow nature of these
345 frequencies and could also be due to some form of traveling oscillatory component (Muller et
346 al., 2018) from posterior temporal areas.

347 Our findings are in line with recent models implicating these posterior portions of temporal
348 lobe in phrase structure building (Flick & Pylkkänen, 2020; Law & Pylkkänen, 2021; Matar et
349 al., 2021; Matchin & Hickok, 2020; Murphy, 2018, 2020); a recent meta-analysis of sign
350 language implicating TOJ and pMTG/pSTS in comprehension (Trettenbrein et al., 2020); and
351 the finding that cross-linguistic (French and Chinese) reading competence is linked to pSTS
352 (Feng et al., 2020), contributing to the neural localization of complex composition (Chomsky
353 et al., 2019; Pietroski, 2018). In particular, evidence from neuroimaging and lesion-deficit
354 mapping indicates a role for pMTG in syntactic comprehension and production (Matchin &
355 Hickok, 2020), while pSTS has been implicated via iEEG in hierarchical syntactic
356 computations (Nelson et al., 2017). Data from brain stimulation implicate postero-middle
357 temporal areas in syntactic processing (Duffau et al., 2014), and a recent *red-boat* study in
358 fMRI implicated a broad portion of pMTG in meaningful phrase composition (Graessner et al.,
359 2021). Impairments in grammaticality judgments have primarily been linked to posterior
360 temporal lobe damage (Wilson & Saygin, 2004). Lastly, widespread monotonic fronto-
361 temporal language network gamma power increases over the course of sentence reading
362 have been documented in iEEG (Fedorenko et al., 2016); our findings isolate a more specific
363 site in the network responsible for the core compositional operator underlying sentence
364 comprehension.

365 We also discovered greater functional connectivity between pSTS-TOJ and both temporal
366 pole and pars triangularis after the presentation of the phrase-licensing nominal (Fig. 5). White
367 matter atlas consultation reveals that the subcortical distribution of responses to semantic
368 stimuli reflects the continuous and homogenous ventral course of functional information in the
369 deep white matter of the temporal lobe, from TOJ, ascending to white matter underneath the
370 posterior two-thirds of IFG (Sarubbo et al., 2020). These ventral workflow pathways subserve
371 our regions of interest (temporal pole; TOJ; IFG). In addition, arcuate fasciculus is classically
372 implicated in connectivity between pSTS-TOJ and pars triangularis (Figley et al., 2017;
373 Glasser & Rilling, 2008). In relation to current findings and frameworks, it is possible that the
374 formation of phrase structure in pSTS-TOJ feeds categorial information (e.g. phrase type) to
375 interpretation interfaces in ATL and memory/control interfaces in pars triangularis (a form of
376 “spell-out”). One such piece of information encoded via PLV would be the phrase
377 category/label (Adger, 2012; Murphy, 2015a; Murphy & Shim, 2020). These results may point
378 to a degree of top-down control from pars triangularis on initial phrase construction in pSTS-
379 TOJ (Hagoort et al., 2009). The more precise computational role of such connectivity metrics
380 requires further empirical, and conceptual, advances.

381 Inhibition of a portion of left posterior temporal lobe (pSTS, pSTG and temporo-parietal
382 junction) selectively impairs the ability to produce appropriate functional morphemes for

383 particular hierarchical relations, but does not effect any other sub-linguistic process such as
384 semantic or lexical retrieval (Lee et al., 2018). Our data are compatible with the idea that in
385 connection with other areas, such as IFG (Baggio & Hagoort, 2011; Zaccarella et al., 2021),
386 pSTS-TOJ contributes to both morphological and phrasal unification (Jackendoff & Audring,
387 2020; Rizzi, 2016). Our results are concordant with a division between sensitivity to non-local
388 dependency structure (in left anterior temporal pole and IFG) and sensitivity to phrase
389 structure (in left pSTG) (Lopopolo et al., 2021). Data from sEEG comparing noun phrases and
390 acoustically-matched, identical words acting as verb phrases (with the latter demanding richer
391 syntactic structure) reveals greater high gamma activity in MTG and STG in the coding of
392 complex syntax (Artoni et al., 2020). This points to partial spatial overlap with our composition
393 effects, in compliance with the idea that the re-application of recursive hierarchical structure
394 generation calls upon the same basic compositional operator (i.e., that the computation
395 implicated in forming verb phrases is the same operation that forms “red boat”).

396 While we did not find composition effects in inferior parietal lobule (in particular, angular gyrus),
397 and had good electrode coverage here, this may be due to this region’s role in higher-order
398 semantic processing (e.g. thematic role assignment, discourse structure) and event structure
399 (Boylan et al., 2015). For instance, there is a range of evidence, including from intracranial
400 recordings, that taxonomic conceptual relationships are encoded in ATL, while thematic
401 relationships are encoded in angular gyrus (Davis & Yee, 2019; Thye et al., 2021).

402 Given the nature of our stimuli, we can make direct claims about semantic composition, and
403 we suspect that portions of pSTS-TOJ are also implicated in minimal syntax, however the
404 dynamics of the syntax network may differ from that of the semantic compositional network.
405 Overall, our results contribute to isolating the neural signatures of basic phrase structure
406 composition, an elementary computational procedure of natural language and potentially a
407 species-defining property (Friederici et al., 2017; Murphy, 2019; Murphy et al., 2021), and we
408 hope that future intracranial research can expand on our findings.

409

410 **Materials and Methods**

411 *Participants*: 19 patients (10 male, 18-41 years, IQ 97 ± 12 , 2 left-handed) participated in the
412 experiment after written informed consent was obtained. All were native English speakers. All
413 experimental procedures were reviewed and approved by the Committee for the Protection of
414 Human Subjects (CPHS) of the University of Texas Health Science Center at Houston as
415 Protocol Number HSC-MS-06-0385.

416 Electrode Implantation and Data Recording: Data were acquired from either subdural grid
417 electrodes (SDEs; 6 patients) or stereotactically placed depth electrodes (sEEGs; 12 patients)
418 (Fig. 1B). SDEs were subdural platinum-iridium electrodes embedded in a silicone elastomer
419 sheet (PMT Corporation; top-hat design; 3mm diameter cortical contact), and were surgically
420 implanted via a craniotomy (Conner et al., 2011; Pieters et al., 2013; Tandon, 2012; Tong et
421 al., 2020). sEEGs were implanted using a Robotic Surgical Assistant (ROSA; Medtech,
422 Montpellier, France) (Rollo et al., 2020; Tandon et al., 2019). Each sEEG probe (PMT
423 corporation, Chanhassen, Minnesota) was 0.8mm in diameter and had 8-16 electrode
424 contacts. Each contact was a platinum-iridium cylinder, 2.0mm in length and separated from
425 the adjacent contact by 1.5-2.43mm. Each patient had 12-20 such probes implanted.
426 Following surgical implantation, electrodes were localized by co-registration of pre-operative
427 anatomical 3T MRI and post-operative CT scans in AFNI (Cox, 1996). Electrode positions
428 were projected onto a cortical surface model generated in FreeSurfer (Dale et al., 1999), and
429 displayed on the cortical surface model for visualization (Pieters et al., 2013). Intracranial data
430 were collected during research experiments starting on the first day after electrode
431 implantation for sEEGs and two days after implantation for SDEs. Data were digitized at 2 kHz
432 using the NeuroPort recording system (Blackrock Microsystems, Salt Lake City, Utah),
433 imported into Matlab, initially referenced to the white matter channel used as a reference for
434 the clinical acquisition system and visually inspected for line noise, artifacts and epileptic
435 activity. Electrodes with excessive line noise or localized to sites of seizure onset were
436 excluded. Each electrode was re-referenced to the common average of the remaining
437 channels. Trials contaminated by inter-ictal epileptic spikes, saccade artefacts and trials in
438 which participants responded incorrectly were discarded.

439 Stimuli and Experimental Design: Participants were presented with two-word auditory
440 phrases, grouped by three conditions: Adjective-Noun (“red boat”), Adjective-Pseudoword
441 (“red neub”), Pseudoword-Noun (“zuik boat”). Since these pseudoword phrases include
442 phonologically viable nonwords, differences in the second position of the phrase between
443 these items and the grammatical noun phrases are likely a result of compositional processing.
444 While most previous studies have presented a licensable noun, our inclusion of the Adjective-
445 Pseudoword condition further isolates composition and reduces predictability. To ensure
446 attention was maintained, after each trial participants were shown a colored drawing and
447 asked to press a button indicating whether the picture matched the phrase they had just heard.
448 Participants were told to respond positively only when the picture fully matched the phrase
449 (e.g. the phrase “red boat” followed by a picture of a red car, or a blue boat, would be negative).
450 Auditory and visual stimuli were recruited from previous *red-boat* experiments (Bemis &
451 Pylkkänen, 2013b).

452 A fixation cross was presented in the centre of the screen for 700ms followed by the first word
453 and 800ms later the second word was presented. 1600ms after the onset of the second word
454 the picture was presented, and 1400ms after picture presentation participants were prompted
455 to respond (Fig. 1A). Following their response, a blank screen was shown for 1500ms. Stimuli
456 were presented in a pseudorandom order, with no repetition amongst items. The number of
457 trials per block across the full experiment was as follows: Adjective-Noun (80), Pseudoword-
458 Noun (40), Adjective-Pseudoword (40). All patients undertook 2 blocks. Half of the Adjective-
459 Noun trials matched the picture presented (i.e. “red boat” was heard by the patient, and a
460 picture of a red boat was then presented), and the other half did not match. 6 adjectives were
461 used: black, blue, brown, green, pink, red (length M: 4.3, SD: 0.7; SUBTLEXus log-frequency
462 3.64). 20 nouns were used: bag, bell, boat, bone, cane, cross, cup, disc, flag, fork, hand, heart,
463 house, key, lamp, leaf, lock, plane, shoe, star (length M: 4.0, SD: 0.6; log-frequency 3.38)
464 (Brysbaert, New, & Keuleers, 2012). 6 pseudowords were used: beeg, cresp, kleg, nar, neub,
465 zuik (length M: 4.0, SD: 0.6). Average stimuli length: Adjectives (420 ms), Nouns (450 ms),
466 Pseudowords (430ms).

467 Stimuli were presented using Psychtoolbox (Kleiner et al., 2007) on a 15.4” LCD screen
468 positioned at eye-level, 2-3’ from the patient. Auditory stimuli were presented using stereo
469 speakers (44.1 kHz, MacBook Pro 2015).

470 *Signal Analysis:* A total of 3458 electrode contacts were implanted in these patients; 2135 of
471 these were included for analysis after excluding channels proximal to the seizure onset zone
472 or exhibiting excessive inter-ictal spikes or line noise. Analyses were performed by first
473 bandpass filtering the raw data of each electrode into broadband gamma activity (BGA; 70–
474 150 Hz) following removal of line noise and its harmonics (zero-phase 2nd order Butterworth
475 band-stop filters). Electrodes were also visually inspected for saccade artefacts. A frequency
476 domain bandpass Hilbert transform (paired sigmoid flanks with half-width 1.5 Hz) was applied
477 and the analytic amplitude was smoothed (Savitzky-Golay FIR, 3rd order, frame length of
478 251ms; Matlab 2019b, Mathworks, Natick, MA). BGA was defined as percentage change from
479 baseline level; -500 to -100ms before the presentation of the first word in each trial. Periods
480 of significant activation were tested using a one-tailed t-test at each time point and were
481 corrected for multiple comparisons with a Benjamini-Hochberg false detection rate (FDR)
482 threshold of $q < 0.05$. For the grouped analysis, all electrodes were averaged within each
483 subject and then the between-subject averages were used.

484 To provide statistically robust and topologically precise estimates of BGA, and to account for
485 variations in sampling density, population-level representations were created using surface-
486 based mixed-effects multilevel analysis (SB-MEMA) (Conner et al., 2011; Fischl et al., 1999;

487 Kadipasaoglu et al., 2014; Kadipasaoglu et al., 2015). This method accounts for sparse
488 sampling, outlier inferences, as well as intra- and inter-subject variability to produce population
489 maps of cortical activity. A geodesic Gaussian smoothing filter (3mm full-width at half-
490 maximum) was applied. Significance levels were computed at a corrected alpha-level of 0.01
491 using family-wise error rate corrections for multiple comparisons. The minimum criterion for
492 the family-wise error rate was determined by white-noise clustering analysis (Monte Carlo
493 simulations, 5000 iterations) of data with the same dimension and smoothness as that
494 analyzed (Kadipasaoglu et al., 2014). Results were further restricted to regions with at least
495 three patients contributing to coverage and BGA percent change exceeding 5%.

496 Anatomical groups of electrodes were delineated, firstly, through indexing electrodes to the
497 closest node on the standardized cortical surface (Saad & Reynolds, 2012), and secondly,
498 through grouping channels into parcellations determined by Human Connectome Project
499 (HCP) space (Glasser et al., 2016). Parametric statistics were used since HCP regions of
500 interest contained >30 electrodes. When contrasting experimental conditions, two-sided
501 paired t-tests were evaluated at each time point for each region and significance levels were
502 computed at $q < 0.01$ using an FDR correction for multiple comparisons.

503 To generate event-related potentials (ERPs), the raw data were band pass filtered (0.1–50
504 Hz). Trials were averaged together and the resultant waveform was smoothed (Savitzky-Golay
505 FIR, third-order, frame length of 251ms). To account for differences in polarity between
506 electrodes, ERPs were converted to root mean square (RMS), using a 50ms sliding window.
507 All electrodes were averaged within each subject, within ROI, and then the between subject
508 averages were used.

509 There is increasing evidence that the phase of activation across distributed neural populations
510 correlates with distinct underlying neural processes from the amplitude (Buzsáki, 2019; Fries,
511 2015; Sauseng & Klimesch, 2008). We investigated the influence of lexicality and phrase
512 construction on inter-trial phase coherence (ITC). Phase information was extracted from the
513 band-pass filtered data (zero-phase 3rd order Butterworth band-pass filter) using a Hilbert
514 transform. ITC was calculated as the circular mean (absolute vector length) of instantaneous
515 phase of stimulus-aligned trials computed as the median value of 10 iterations of a random
516 50% of trials.

517 To explore the functional connectivity between regions of interest, we used a generalized
518 phase-locking analysis to estimate the dominant spatio-temporal distributions of field activity,
519 and the strength of the coupling between them. Phase information was extracted from the
520 down-sampled (200 Hz) and wide band-pass filtered data (3–50 Hz; zero-phase 8th order
521 Butterworth band-pass filter) using the ‘generalized phase’ method (Davis et al., 2020) with a

522 single-sided Fourier transform approach (Marple, 1999). This method captures the phase of
523 the predominant fluctuations in the wideband signal and minimizes filter-related distortion of
524 the waveform. PLV was calculated as the circular mean (absolute vector length) of the
525 instantaneous phase difference between each electrode pair at each time point and baselined
526 to the period -500 to -100 ms before onset of the first word. Statistics were calculated using
527 the mean PLV of correctly answered trials between 0 to 500ms after second word onset,
528 comparing against a null distribution generated by randomly re-pairing trial recordings across
529 the electrode pairs 500 times. Significant PLV was accepted at a threshold of $p < 0.05$.

530

531 **Acknowledgements**

532 We express our gratitude to all the patients who participated in this study; the neurologists at
533 the Texas Comprehensive Epilepsy Program who participated in the care of these patients;
534 and the nurses and technicians in the Epilepsy Monitoring Unit at Memorial Hermann Hospital
535 who helped make this research possible. This work was supported by the National Institute of
536 Neurological Disorders and Stroke NS098981. Human subjects: Patients participated in the
537 experiments after written informed consent was obtained. All experimental procedures were
538 reviewed and approved by the Committee for the Protection of Human Subjects (CPHS) of
539 the University of Texas Health Science Center at Houston as Protocol Number: HSC-MS-06-
540 0385.

541 **References**

- 542 Adger, D. (2012). *A Syntax of Substance*. <https://doi.org/10.7551/mitpress/9780262018616.001.0001>
- 543 Amunts, K., & Zilles, K. (2015). Architectonic Mapping of the Human Brain beyond Brodmann. *Neuron*, 88(6),
544 1086–1107. <https://doi.org/10.1016/j.neuron.2015.12.001>
- 545 Antonucci, S., Beeson, P., Labiner, D., & Rapcsak, S. (2008). Lexical retrieval and semantic knowledge in
546 patients with left inferior temporal lobe lesions. *Aphasiology*, 22(3), 281–304.
547 <https://doi.org/10.1080/02687030701294491>
- 548 Artoni, F., D’Orio, P., Catricalà, E., Conca, F., Bottoni, F., Pelliccia, V., ... Moro, A. (2020). High gamma response
549 tracks different syntactic structures in homophonous phrases. *Scientific Reports*, 10(1), 7537.
550 <https://doi.org/10.1038/s41598-020-64375-9>
- 551 Arya, R. (2019). Similarity of spatiotemporal dynamics of language-related ECoG high-gamma modulation in
552 Japanese and English speakers. *Clinical Neurophysiology*, 130(8), 1403–1404.
553 <https://doi.org/10.1016/j.clinph.2019.05.006>
- 554 Baggio, G., & Hagoort, P. (2011). The balance between memory and unification in semantics: A dynamic account
555 of the N400. *Language and Cognitive Processes*, 26(9), 1338–1367.
556 <https://doi.org/10.1080/01690965.2010.542671>
- 557 Bastiaansen, M., & Hagoort, P. (2015). Frequency-based Segregation of Syntactic and Semantic Unification
558 during Online Sentence Level Language Comprehension. *Journal of Cognitive Neuroscience*, 27(11),
559 2095–2107. https://doi.org/10.1162/jocn_a_00829
- 560 Bemis, D. K., & Pykkänen, L. (2013). Basic linguistic composition recruits the left anterior temporal lobe and left
561 angular gyrus during both listening and reading. *Cerebral Cortex*. <https://doi.org/10.1093/cercor/bhs170>
- 562 Bemis, Douglas K., & Pykkänen, L. (2011). Simple composition: A magnetoencephalography investigation into
563 the comprehension of minimal linguistic phrases. *Journal of Neuroscience*, 31(8), 2801–2814.
564 <https://doi.org/10.1523/JNEUROSCI.5003-10.2011>
- 565 Bemis, Douglas K., & Pykkänen, L. (2013). Combination across domains: An MEG investigation into the
566 relationship between mathematical, pictorial, and linguistic processing. *Frontiers in Psychology*, 3, 583.
567 <https://doi.org/10.3389/fpsyg.2012.00583>
- 568 Benítez-Burraco, A., & Murphy, E. (2019). Why Brain Oscillations Are Improving Our Understanding of Language.
569 *Frontiers in Behavioral Neuroscience*. <https://doi.org/10.3389/fnbeh.2019.00190>

- 570 Berwick, R. C., Stabler, E. P., Berwick, R. C., & Stabler, E. P. (2019). Minimalist parsing. In *Minimalist Parsing*.
571 <https://doi.org/10.1093/oso/9780198795087.003.0001>
- 572 Boylan, C., Trueswell, J. C., & Thompson-Schill, S. L. (2015). Compositionality and the angular gyrus: A multi-
573 voxel similarity analysis of the semantic composition of nouns and verbs. *Neuropsychologia*, *78*, 130–141.
574 <https://doi.org/10.1016/j.neuropsychologia.2015.10.007>
- 575 Bozic, M., Fonteneau, E., Su, L., & Marslen-Wilson, W. D. (2015). Grammatical analysis as a distributed
576 neurobiological function. *Human Brain Mapping*, *36*(3), 1190–1201. <https://doi.org/10.1002/hbm.22696>
- 577 Brennan, J., & Pylkkänen, L. (2012). The time-course and spatial distribution of brain activity associated with
578 sentence processing. *NeuroImage*, *60*(2), 1139–1148. <https://doi.org/10.1016/j.neuroimage.2012.01.030>
- 579 Brennan, J. R., Stabler, E. P., Van Wagenen, S. E., Luh, W. M., & Hale, J. T. (2016). Abstract linguistic structure
580 correlates with temporal activity during naturalistic comprehension. *Brain and Language*, *157–158*, 81–94.
581 <https://doi.org/10.1016/j.bandl.2016.04.008>
- 582 Brysbaert, M., New, B., & Keuleers, E. (2012). Adding part-of-speech information to the SUBTLEX-US word
583 frequencies. *Behavior Research Methods*, *44*(4), 991–997. <https://doi.org/10.3758/s13428-012-0190-4>
- 584 Buzsáki, G. (2019). *The Brain from Inside Out*. <https://doi.org/10.1093/oso/9780190905385.001.0001>
- 585 Buzsáki, G., & Watson, B. O. (2012). Brain rhythms and neural syntax: implications for efficient coding of
586 cognitive content and neuropsychiatric disease. *Dialogues in Clinical Neuroscience*, *14*(4), 345–367.
587 <https://doi.org/10.31887/DCNS.2012.14.4/gbuzsaki>
- 588 Canolty, R. T., Soltani, M., Dalal, S. S., Edwards, E., Dronkers, N. F., Nagarajan, S. S., ... Knight, R. T. (2007).
589 Spatiotemporal Dynamics of Word Processing in the Human Brain. *Frontiers in Neuroscience*, *1*(1), 185–
590 196. <https://doi.org/10.3389/neuro.01.1.1.014.2007>
- 591 Cazzoli, D., Kaufmann, B. C., Paladini, R. E., Müri, R. M., Nef, T., & Nyffeler, T. (2021). Anterior insula and
592 inferior frontal gyrus: where ventral and dorsal visual attention systems meet. *Brain Communications*.
593 <https://doi.org/10.1093/braincomms/fcaa220>
- 594 Chomsky, N. (1995). *The Minimalist Program*. Cambridge, MA: MIT Press.
- 595 Chomsky, N., Gallego, A. J., & Ott, D. (2019). Generative grammar and the faculty of language: insights,
596 questions, and challenges. *Catalan Journal of Linguistics Special Issue*, 226–261.
- 597 Conner, C. R., Ellmore, T. M., Pieters, T. A., di Sano, M. A., & Tandon, N. (2011). Variability of the relationship
598 between electrophysiology and BOLD-fMRI across cortical regions in humans. *Journal of Neuroscience*,

- 599 31, 12855–12865. <https://doi.org/10.1523/JNEUROSCI.1457-11.2011>
- 600 Conner, C. R., Kadipasaoglu, C. M., Shouval, H. Z., Hickok, G., & Tandon, N. (2019). Network dynamics of
601 Broca's area during word selection. *PLoS ONE*, 14(12), 1–30. <https://doi.org/10.1371/journal.pone.0225756>
- 602 Cox, R. W. (1996). AFNI: Software for Analysis and Visualization of Functional Magnetic Resonance
603 Neuroimages. *Computers and Biomedical Research*, 29(3), 162–173.
604 <https://doi.org/10.1006/cbmr.1996.0014>
- 605 Dale, A. M., Fischl, B., & Sereno, M. I. (1999). Cortical Surface-Based Analysis: I. Segmentation and Surface
606 Reconstruction. *NeuroImage*, 9(2), 179–194. <https://doi.org/10.1006/nimg.1998.0395>
- 607 Davis, C. P., & Yee, E. (2019). Features, labels, space, and time: factors supporting taxonomic relationships in
608 the anterior temporal lobe and thematic relationships in the angular gyrus. *Language, Cognition and
609 Neuroscience*, 34(10), 1347–1357.
- 610 Davis, Z. W., Muller, L., Martinez-Trujillo, J., Sejnowski, T., & Reynolds, J. H. (2020). Spontaneous travelling
611 cortical waves gate perception in behaving primates. *Nature*, 587(7834), 432–436.
612 <https://doi.org/10.1038/s41586-020-2802-y>
- 613 Ding, N., Melloni, L., Zhang, H., Tian, X., & Poeppel, D. (2016). Cortical tracking of hierarchical linguistic
614 structures in connected speech. *Nature Neuroscience*, 19(1), 158–164. <https://doi.org/10.1038/nn.4186>
- 615 Duffau, H., Moritz-Gasser, S., & Mandonnet, E. (2014). A re-examination of neural basis of language processing:
616 Proposal of a dynamic hodotopical model from data provided by brain stimulation mapping during picture
617 naming. *Brain and Language*, 131, 1–10. <https://doi.org/10.1016/j.bandl.2013.05.011>
- 618 Fedorenko, E., Scott, T. L., Brunner, P., Coon, W. G., Pritchett, B., Schalk, G., & Kanwisher, N. (2016). Neural
619 correlate of the construction of sentence meaning. *Proceedings of the National Academy of Sciences of the
620 United States of America*, 113(41), E6256–E6262. <https://doi.org/10.1073/pnas.1612132113>
- 621 Feng, X., Altarelli, I., Monzalvo, K., Ding, GuoshengRamus, F., Shu, H., Dehaene, S., ... Dehaene-Lambertz, G.
622 (2020). A universal reading network and its modulation by writing system and reading ability in French and
623 Chinese children. *ELife*, 9, e54591.
- 624 Figley, T. D., Mortazavi Moghadam, B., Bhullar, N., Kornelsen, J., Courtney, S. M., & Figley, C. R. (2017).
625 Probabilistic white matter atlases of human auditory, basal ganglia, language, precuneus, sensorimotor,
626 visual and visuospatial networks. *Frontiers in Human Neuroscience*, 11(June), 1–12.
627 <https://doi.org/10.3389/fnhum.2017.00306>

- 628 Fischl, B., Sereno, M. I., & Dale, A. M. (1999). Cortical surface-based analysis: II. Inflation, flattening, and a
629 surface-based coordinate system. *NeuroImage*, 9, 195–207. <https://doi.org/10.1006/nimg.1998.0396>
- 630 Flick, G., Oseki, Y., Kaczmarek, A. R., Al Kaabi, M., Marantz, A., & Pylkkänen, L. (2018). Building words and
631 phrases in the left temporal lobe. *Cortex*, 106, 213–236. <https://doi.org/10.1016/j.cortex.2018.06.004>
- 632 Flick, G., & Pylkkänen, L. (2020). Isolating syntax in natural language: MEG evidence for an early contribution of
633 left posterior temporal cortex. *Cortex*, 127, 42–57. <https://doi.org/10.1016/j.cortex.2020.01.025>
- 634 Flinker, A., Chang, E. F., Barbaro, N. M., Berger, M. S., & Knight, R. T. (2011). Sub-centimeter language
635 organization in the human temporal lobe. *Brain and Language*, 117(3), 103–109.
636 <https://doi.org/10.1016/j.bandl.2010.09.009>
- 637 Forseth, K. J., Kadipasaoglu, C. M., Conner, C. R., Hickok, G., Knight, R. T., & Tandon, N. (2018). A lexical
638 semantic hub for heteromodal naming in middle fusiform gyrus. *Brain*, 141(7), 2112–2126.
639 <https://doi.org/10.1093/brain/awy120>
- 640 Friederici, A. D., Chomsky, N., Berwick, R. C., Moro, A., & Bolhuis, J. J. (2017). Language, mind and brain.
641 *Nature Human Behaviour*, 1(10), 713–722. <https://doi.org/10.1038/s41562-017-0184-4>
- 642 Fries, P. (2015). Rhythms for Cognition: Communication through Coherence. *Neuron*, 88, 220–235.
643 <https://doi.org/10.1016/j.neuron.2015.09.034>
- 644 Gastaldon, S., Arcara, G., Navarrete, E., & Peressotti, F. (2020). Commonalities in alpha and beta neural
645 desynchronizations during prediction in language comprehension and production. *Cortex*, 133, 328–345.
646 <https://doi.org/10.1016/j.cortex.2020.09.026>
- 647 Glasser, M. F., Coalson, T. S., Robinson, E. C., Hacker, C. D., Harwell, J., Yacoub, E., ... Van Essen, D. C.
648 (2016). A multi-modal parcellation of human cerebral cortex. *Nature*, 536(7615), 171–178.
649 <https://doi.org/10.1038/nature18933>
- 650 Glasser, M. F., & Rilling, J. K. (2008). DTI Tractography of the Human Brain's Language Pathways. *Cerebral*
651 *Cortex*, 18(11), 2471–2482. <https://doi.org/10.1093/cercor/bhn011>
- 652 Graessner, A., Zaccarella, E., & Hartwigsen, G. (2021). Differential contributions of left-hemispheric language
653 regions to basic semantic composition. *Brain Structure and Function*. [https://doi.org/10.1007/s00429-020-](https://doi.org/10.1007/s00429-020-02196-2)
654 [02196-2](https://doi.org/10.1007/s00429-020-02196-2)
- 655 Hagoort, P. (2003). How the brain solves the binding problem for language: A neurocomputational model of
656 syntactic processing. *NeuroImage*, 20, S18–S29. <https://doi.org/10.1016/j.neuroimage.2003.09.013>

- 657 Hagoort, P. (2004). Integration of Word Meaning and World Knowledge in Language Comprehension. *Science*,
658 304(5669), 438–441. <https://doi.org/10.1126/science.1095455>
- 659 Hagoort, P. (2005). On Broca, brain, and binding: A new framework. *Trends in Cognitive Sciences*.
660 <https://doi.org/10.1016/j.tics.2005.07.004>
- 661 Hagoort, P. (2013). MUC (Memory, Unification, Control) and beyond. *Frontiers in Psychology*, 4.
662 <https://doi.org/10.3389/fpsyg.2013.00416>
- 663 Hagoort, P. (2017). The core and beyond in the language-ready brain. *Neuroscience & Biobehavioral Reviews*,
664 81, 194–204. <https://doi.org/10.1016/j.neubiorev.2017.01.048>
- 665 Hagoort, P. (2020). The meaning-making mechanism(s) behind the eyes and between the ears. *Philosophical*
666 *Transactions of the Royal Society of London. Series B, Biological Sciences*, 375(1791), 20190301.
667 <https://doi.org/10.1098/rstb.2019.0301>
- 668 Hagoort, P., Baggio, G., & Willems, R. M. (2009). Semantic unification. In M. S. Gazzaniga (Ed.), *The Cognitive*
669 *Neurosciences* (4th ed., pp. 819–836). MIT Press.
- 670 Hagoort, P., & Indefrey, P. (2014). The Neurobiology of Language Beyond Single Words. *Annual Review of*
671 *Neuroscience*, 37(1), 347–362. <https://doi.org/10.1146/annurev-neuro-071013-013847>
- 672 Hovsepian, S., Olasagasti, I., & Giraud, A.-L. (2020). Combining predictive coding and neural oscillations
673 enables online syllable recognition in natural speech. *Nature Communications*, 11(1), 3117.
674 <https://doi.org/10.1038/s41467-020-16956-5>
- 675 Humphries, C., Binder, J. R., Medler, D. A., & Liebenthal, E. (2006). Syntactic and semantic modulation of neural
676 activity during auditory sentence comprehension. *Journal of Cognitive Neuroscience*.
677 <https://doi.org/10.1162/jocn.2006.18.4.665>
- 678 Irimia, A., Van Horn, J. D., & Halgren, E. (2012). Source cancellation profiles of electroencephalography and
679 magnetoencephalography. *NeuroImage*, 59(3), 2464–2474.
680 <https://doi.org/10.1016/j.neuroimage.2011.08.104>
- 681 Jackendoff, R., & Audring, J. (2020). *The Texture of the Lexicon: Relational Morphology and the Parallel*
682 *Architecture*. Oxford: Oxford University Press.
- 683 Jensen, O., Spaak, E., & Zumer, J. M. (2019). Human brain oscillations: From physiological mechanisms to
684 analysis and cognition. In *Magnetoencephalography: From Signals to Dynamic Cortical Networks: Second*
685 *Edition*. https://doi.org/10.1007/978-3-030-00087-5_17

- 686 Johnson, E. L., Kam, J. W. Y., Tzovara, A., & Knight, R. T. (2020). Insights into human cognition from intracranial
687 EEG: A review of audition, memory, internal cognition, and causality. *Journal of Neural Engineering*, 17(5),
688 051001. <https://doi.org/10.1088/1741-2552/abb7a5>
- 689 Kadipasaoglu, C. M., Baboyan, V. G., Conner, C. R., Chen, G., Saad, Z. S., & Tandon, N. (2014). Surface-based
690 mixed effects multilevel analysis of grouped human electrocorticography. *NeuroImage*, 101, 215–224.
691 <https://doi.org/10.1016/j.neuroimage.2014.07.006>
- 692 Kadipasaoglu, Cihan M., Forseth, K., Whaley, M., Conner, C. R., Rollo, M. J., Baboyan, V. G., & Tandon, N.
693 (2015). Development of grouped icEEG for the study of cognitive processing. *Frontiers in Psychology*,
694 6(1008). <https://doi.org/10.3389/fpsyg.2015.01008>
- 695 Keitel, A., Gross, J., & Kayser, C. (2018). Perceptually relevant speech tracking in auditory and motor cortex
696 reflects distinct linguistic features. *PLOS Biology*, 16(3), e2004473.
697 <https://doi.org/10.1371/journal.pbio.2004473>
- 698 Keitel, A., Ince, R. A. A., Gross, J., & Kayser, C. (2017). Auditory cortical delta-entrainment interacts with
699 oscillatory power in multiple fronto-parietal networks. *NeuroImage*, 147, 32–42.
700 <https://doi.org/10.1016/j.neuroimage.2016.11.062>
- 701 Kleiner, M., Brainard, D., Pelli, D., Ingling, A., Murray, R., & Broussard, C. (2007). What's new in psychtoolbox-3.
702 *Perception*, 36(14), 1–16.
- 703 Kucyi, A., & Parvizi, J. (2020). Pupillary Dynamics Link Spontaneous and Task-Evoked Activations Recorded
704 Directly from Human Insula. *The Journal of Neuroscience*, 40(32), 6207–6218.
705 <https://doi.org/10.1523/JNEUROSCI.0435-20.2020>
- 706 Lambon Ralph, M. A., Ehsan, S., Baker, G. A., & Rogers, T. T. (2012). Semantic memory is impaired in patients
707 with unilateral anterior temporal lobe resection for temporal lobe epilepsy. *Brain*, 135(1), 242–258.
708 <https://doi.org/10.1093/brain/awr325>
- 709 Lau, E., Stroud, C., Plesch, S., & Phillips, C. (2006). The role of structural prediction in rapid syntactic analysis.
710 *Brain and Language*, 98(1), 74–88. <https://doi.org/10.1016/j.bandl.2006.02.003>
- 711 Law, R., & Pykkänen, L. (2021). Lists with and without Syntax: A New Approach to Measuring the Neural
712 Processing of Syntax. *The Journal of Neuroscience*, 41(10), 2186–2196.
713 <https://doi.org/10.1523/JNEUROSCI.1179-20.2021>
- 714 Lee, D. K., Fedorenko, E., Simon, M. V., Curry, W. T., Nahed, B. V., Cahill, D. P., & Williams, Z. M. (2018).
715 Neural encoding and production of functional morphemes in the posterior temporal lobe. *Nature*

- 716 *Communications*, 9, 1877. <https://doi.org/10.1038/s41467-018-04235-3>
- 717 Leivada, E., & Murphy, E. (2021). Mind the (terminological) gap: 10 misused, ambiguous, or polysemous terms in
718 linguistics. *Ampersand*, 8, 100073. <https://doi.org/10.1016/j.amper.2021.100073>
- 719 Leszczyński, M., Barczak, A., Kajikawa, Y., Ulbert, I., Falchier, A. Y., Tal, I., ... Schroeder, C. E. (2020).
720 Dissociation of broadband high-frequency activity and neuronal firing in the neocortex. *Science Advances*,
721 6(33), eabb0977. <https://doi.org/10.1126/sciadv.abb0977>
- 722 Lewis, A. G., Schoffelen, J.-M., Schriefers, H., & Bastiaansen, M. (2016). A Predictive Coding Perspective on
723 Beta Oscillations during Sentence-Level Language Comprehension. *Frontiers in Human Neuroscience*, 10,
724 83. <https://doi.org/10.3389/fnhum.2016.00085>
- 725 Lopopolo, A., van den Bosch, A., Petersson, K.-M., & Willems, R. M. (2021). Distinguishing Syntactic Operations
726 in the Brain: Dependency and Phrase-Structure Parsing. *Neurobiology of Language*, 2(1), 152–175.
727 https://doi.org/10.1162/nol_a_00029
- 728 Mai, G., Minett, J. W., & Wang, W. S.-Y. (2016). Delta, theta, beta, and gamma brain oscillations index levels of
729 auditory sentence processing. *NeuroImage*, 133, 516–528.
730 <https://doi.org/10.1016/j.neuroimage.2016.02.064>
- 731 Marko, M., Cimrová, B., & Riečanský, I. (2019). Neural theta oscillations support semantic memory retrieval.
732 *Scientific Reports*, 9(1), 17667. <https://doi.org/10.1038/s41598-019-53813-y>
- 733 Marple, L. (1999). Computing the discrete-time “analytic” signal via FFT. *IEEE Transactions on Signal*
734 *Processing*, 47(9), 2600–2603.
- 735 Martin, S., Millán, J. del R., Knight, R. T., & Pasley, B. N. (2019). The use of intracranial recordings to decode
736 human language: Challenges and opportunities. *Brain and Language*, 193, 73–83.
737 <https://doi.org/10.1016/j.bandl.2016.06.003>
- 738 Matar, S., Dirani, J., Marantz, A., & Pykkänen, L. (2021). Left posterior temporal cortex is sensitive to syntax
739 within conceptually matched Arabic expressions. *Scientific Reports*, 11(7181).
- 740 Matchin, W., & Hickok, G. (2020). The Cortical Organization of Syntax. *Cerebral Cortex*, 30(3), 1481–1498.
741 <https://doi.org/10.1093/cercor/bhz180>
- 742 Muller, L., Chavane, F., Reynolds, J., & Sejnowski, T. J. (2018). Cortical travelling waves: mechanisms and
743 computational principles. *Nature Reviews Neuroscience*, 19(5), 255–268.
744 <https://doi.org/10.1038/nrn.2018.20>

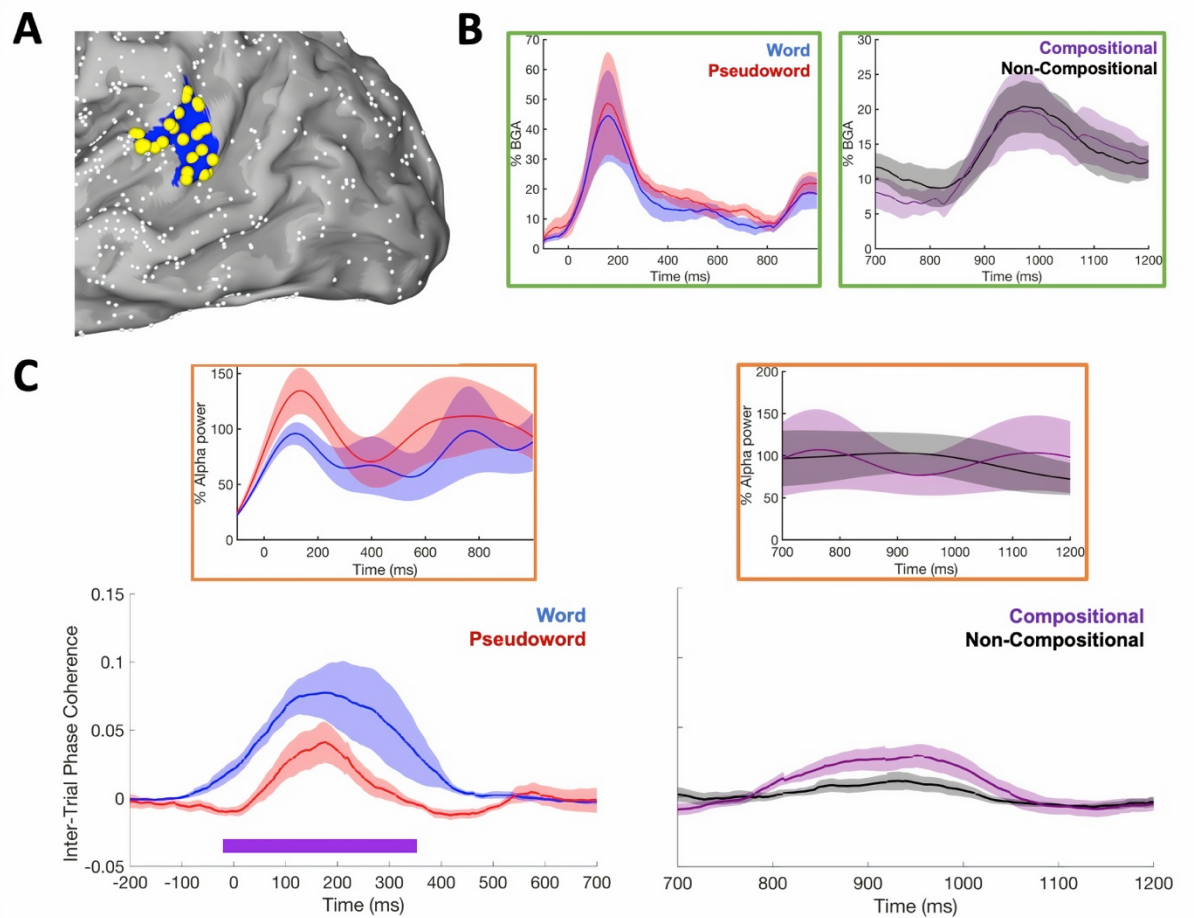
- 745 Murphy, E. (2015a). Labels, cognomes, and cyclic computation: An ethological perspective. *Frontiers in*
746 *Psychology*, 6(715). <https://doi.org/10.3389/fpsyg.2015.00715>
- 747 Murphy, E. (2015b). The brain dynamics of linguistic computation. *Frontiers in Psychology*, 6(1515).
748 <https://doi.org/10.3389/fpsyg.2015.01515>
- 749 Murphy, Elliot. (2015). Labels, cognomes, and cyclic computation: An ethological perspective. *Frontiers in*
750 *Psychology*, 6(715). <https://doi.org/10.3389/fpsyg.2015.00715>
- 751 Murphy, Elliot. (2018). Interfaces (travelling oscillations) + recursion (delta-theta code) = language. In E. Luef &
752 M. Manuela (Eds.), *The Talking Species: Perspectives on the Evolutionary, Neuronal and Cultural*
753 *Foundations of Language* (pp. 251–269). Graz.
- 754 Murphy, Elliot. (2019). No Country for Oldowan Men: Emerging Factors in Language Evolution. *Frontiers in*
755 *Psychology*, 10. <https://doi.org/10.3389/fpsyg.2019.01448>
- 756 Murphy, Elliot. (2020). *The Oscillatory Nature of Language*. Cambridge: Cambridge University Press.
- 757 Murphy, Elliot, Holmes, E., & Friston, K. (2021). Natural language syntax complies with the free-energy principle.
758 *PsyArXiv*. <https://doi.org/doi.org/10.31234/osf.io/r3fcx>
- 759 Murphy, Elliot, & Shim, J.-Y. (2020). Copy invisibility and (non-)categorical labeling. *Linguistic Research*, 37(2),
760 187–215. <https://doi.org/10.17250/khisli.37.2.202006.002>
- 761 Nelson, M. J., El Karoui, I., Giber, K., Yang, X., Cohen, L., Koopman, H., ... Dehaene, S. (2017).
762 Neurophysiological dynamics of phrase-structure building during sentence processing. *Proceedings of the*
763 *National Academy of Sciences of the United States of America*, 114(18), E3669–E3678.
764 <https://doi.org/10.1073/pnas.1701590114>
- 765 Neufeld, C., Kramer, S. E., Lapinskaya, N., Heffner, C. C., Malko, A., & Lau, E. F. (2016). The electrophysiology
766 of basic phrase building. *PLoS ONE*, 11(10), 1–22. <https://doi.org/10.1371/journal.pone.0158446>
- 767 Packard, P. A., Steiger, T. K., Fuentemilla, L., & Bunzeck, N. (2020). Neural oscillations and event-related
768 potentials reveal how semantic congruence drives long-term memory in both young and older humans.
769 *Scientific Reports*. <https://doi.org/10.1038/s41598-020-65872-7>
- 770 Pieters, T. A., Conner, C. R., & Tandon, N. (2013). Recursive grid partitioning on a cortical surface model: an
771 optimized technique for the localization of implanted subdural electrodes. *Journal of Neurosurgery*, 118(5),
772 1086–1097. <https://doi.org/10.3171/2013.2.JNS121450>
- 773 Pietroski, P. M. (2018). Conjoining meanings: Semantics without truth values. In *Conjoining Meanings: Semantics*

- 774 *Without Truth Values*. <https://doi.org/10.1093/oso/9780198812722.001.0001>
- 775 Pobric, G., Jefferies, E., & Lambon Ralph, M. A. (2010). Category-Specific versus Category-General Semantic
776 Impairment Induced by Transcranial Magnetic Stimulation. *Current Biology*, 20(10), 964–968.
777 <https://doi.org/10.1016/j.cub.2010.03.070>
- 778 Prystauka, Y., & Lewis, A. G. (2019). The power of neural oscillations to inform sentence comprehension: A
779 linguistic perspective. *Language and Linguistics Compass*, 13(9). <https://doi.org/10.1111/lnc3.12347>
- 780 Pulvermüller, F., & Grisoni, L. (2020). Semantic prediction in brain and mind. *Trends in Cognitive Sciences*,
781 24(10), 781–784.
- 782 Pykkänen, L. (2020). Neural basis of basic composition: what we have learned from the red-boat studies and
783 their extensions. *Philosophical Transactions of the Royal Society of London. Series B, Biological Sciences*,
784 375(1791), 20190299. <https://doi.org/10.1098/rstb.2019.0299>
- 785 Pykkänen, L., & Brennan, J. (2020). Composition: the neurobiology of syntactic and semantic phrase structure
786 building. In D. Poeppel, G. . Mangun, & M. . Gazzaniga (Eds.), *The Cognitive Neurosciences* (6th ed.).
787 Cambridge, MA: MIT Press.
- 788 Rizzi, L. (2016). Monkey morpho-syntax and merge-based systems. *Theoretical Linguistics*, 42(1–2), 139–145.
789 <https://doi.org/10.1515/tl-2016-0006>
- 790 Rollo, P. S., Rollo, M. J., Zhu, P., Woolnough, O., & Tandon, N. (2020). Oblique trajectory angles in robotic
791 stereo-electroencephalography. *Journal of Neurosurgery*, 1–10. <https://doi.org/10.3171/2020.5.JNS20975>
- 792 Saad, Z. S., & Reynolds, R. C. (2012). SUMA. *NeuroImage*, 62, 768–773.
793 <https://doi.org/10.1016/j.neuroimage.2011.09.016>
- 794 Sarubbo, S., Tate, M., De Benedictis, A., Merler, S., Moritz-Gasser, S., Herbet, G., & Duffau, H. (2020). Mapping
795 critical cortical hubs and white matter pathways by direct electrical stimulation: an original functional atlas of
796 the human brain. *NeuroImage*, 205(September 2019), 116237.
797 <https://doi.org/10.1016/j.neuroimage.2019.116237>
- 798 Sauseng, P., & Klimesch, W. (2008). What does phase information of oscillatory brain activity tell us about
799 cognitive processes? *Neuroscience and Biobehavioral Reviews*, 32, 1001–1013.
800 <https://doi.org/10.1016/j.neubiorev.2008.03.014>
- 801 Schell, M., Zaccarella, E., & Friederici, A. D. (2017). Differential cortical contribution of syntax and semantics: An
802 fMRI study on two-word phrasal processing. *Cortex*, 96, 105–120.

- 803 <https://doi.org/10.1016/j.cortex.2017.09.002>
- 804 Segaert, K., Mazaheri, A., & Hagoort, P. (2018). Binding language: structuring sentences through precisely timed
805 oscillatory mechanisms. *European Journal of Neuroscience*, 48(7), 2651–2662.
806 <https://doi.org/10.1111/ejn.13816>
- 807 Tandon, N. (2012). Mapping of human language. In D. Yoshor & E. Mizrahi (Eds.), *Clinical Brain Mapping* (pp.
808 203–218). McGraw Hill Education.
- 809 Tandon, N., Tong, B. A., Friedman, E. R., Johnson, J. A., Von Allmen, G., Thomas, M. S., ... Thompson, S. A.
810 (2019). Analysis of Morbidity and Outcomes Associated with Use of Subdural Grids vs
811 Stereoelectroencephalography in Patients with Intractable Epilepsy. *JAMA Neurology*, 76, 672–681.
812 <https://doi.org/10.1001/jamaneurol.2019.0098>
- 813 Tanji, K., Suzuki, K., Delorme, A., Shamoto, H., & Nakasato, N. (2005). High-frequency γ -band activity in the
814 basal temporal cortex during picture-naming and lexical-decision tasks. *Journal of Neuroscience*, 25(13),
815 3287–3293. <https://doi.org/10.1523/JNEUROSCI.4948-04.2005>
- 816 Terporten, R., Schoffelen, J. M., Dai, B., Hagoort, P., & Kösem, A. (2019). The Relation between Alpha/Beta
817 Oscillations and the Encoding of Sentence induced Contextual Information. *Scientific Reports*.
818 <https://doi.org/10.1038/s41598-019-56600-x>
- 819 Thye, M., Geller, J., Szaflarski, J. P., & Mirman, D. (2021). Intracranial EEG evidence of functional specialization
820 for taxonomic and thematic relations. *Cortex*. <https://doi.org/10.1016/j.cortex.2021.03.018>
- 821 Tong, B. A., Esquenazi, Y., Johnson, J., Zhu, P., & Tandon, N. (2020). The Brain is Not Flat: Conformal Electrode
822 Arrays Diminish Complications of Subdural Electrode Implantation, A Series of 117 Cases. *World*
823 *Neurosurgery*, 144, e734–e742. <https://doi.org/10.1016/j.wneu.2020.09.063>
- 824 Towle, V. L., Yoon, H.-A., Castelle, M., Edgar, J. C., Biassou, N. M., Frim, D. M., ... Kohrman, M. H. (2008).
825 ECoG gamma activity during a language task: differentiating expressive and receptive speech areas. *Brain*,
826 131(8), 2013–2027. <https://doi.org/10.1093/brain/awn147>
- 827 Trettenbrein, P., Papitto, G., Friederici, A. D., & Zaccarella, E. (2020). Functional neuroanatomy of language
828 without speech: An ALE meta-analysis of sign language. *Human Brain Mapping*, doi.org/10.1002/hbm.25000
- 829 Wang, X., Men, W., Gao, J., Caramazza, A., & Bi, Y. (2020). Two Forms of Knowledge Representations in the
830 Human Brain. *Neuron*, 107(2), 383–393. <https://doi.org/10.1016/j.neuron.2020.04.010>
- 831 Westerlund, M., Kastner, I., Al Kaabi, M., & Pylkkänen, L. (2015). The LATL as locus of composition: MEG

- 832 evidence from English and Arabic. *Brain and Language*, 141, 124–134.
833 <https://doi.org/10.1016/j.bandl.2014.12.003>
- 834 Westerlund, M., & Pylkkänen, L. (2014). The role of the left anterior temporal lobe in semantic composition vs.
835 semantic memory. *Neuropsychologia*, 57(1), 59–70.
836 <https://doi.org/10.1016/j.neuropsychologia.2014.03.001>
- 837 Wilson, S. M., DeMarco, A. T., Henry, M. L., Gesierich, B., Babiak, M., Mandelli, M. L., ... Gorno-Tempini, M. L.
838 (2014). What role does the anterior temporal lobe play in sentence-level processing? neural correlates of
839 syntactic processing in semantic variant primary progressive aphasia. *Journal of Cognitive Neuroscience*,
840 26(5), 970–985. https://doi.org/10.1162/jocn_a_00550
- 841 Wilson, S. M., & Saygin, A. P. (2004). Grammaticality Judgment in Aphasia: Deficits Are Not Specific to Syntactic
842 Structures, Aphasic Syndromes, or Lesion Sites. *Journal of Cognitive Neuroscience*, 16, 238–252.
843 <https://doi.org/10.1162/089892904322984535>
- 844 Woolnough, O., Forseth, K. J., Rollo, P. S., & Tandon, N. (2019). Uncovering the functional anatomy of the
845 human insula during speech. *ELife*, 8, 1–14. <https://doi.org/10.7554/eLife.53086>
- 846 Yi, H. G., Leonard, M. K., & Chang, E. F. (2019). The Encoding of Speech Sounds in the Superior Temporal
847 Gyrus. *Neuron*, 102(6), 1096–1110. <https://doi.org/10.1016/j.neuron.2019.04.023>
- 848 Zaccarella, E., Papitto, G., & Friederici, A. D. (2021). Language and action in Broca's area: Computational
849 differentiation and cortical segregation. *Brain and Cognition*, 147, 105651.
850 <https://doi.org/10.1016/j.bandc.2020.105651>
- 851 Zhang, L., & Pylkkänen, L. (2018). Semantic composition of sentences word by word: MEG evidence for shared
852 processing of conceptual and logical elements. *Neuropsychologia*, 119(April), 392–404.
853 <https://doi.org/10.1016/j.neuropsychologia.2018.08.016>
- 854

855 **Supplementary Figures**

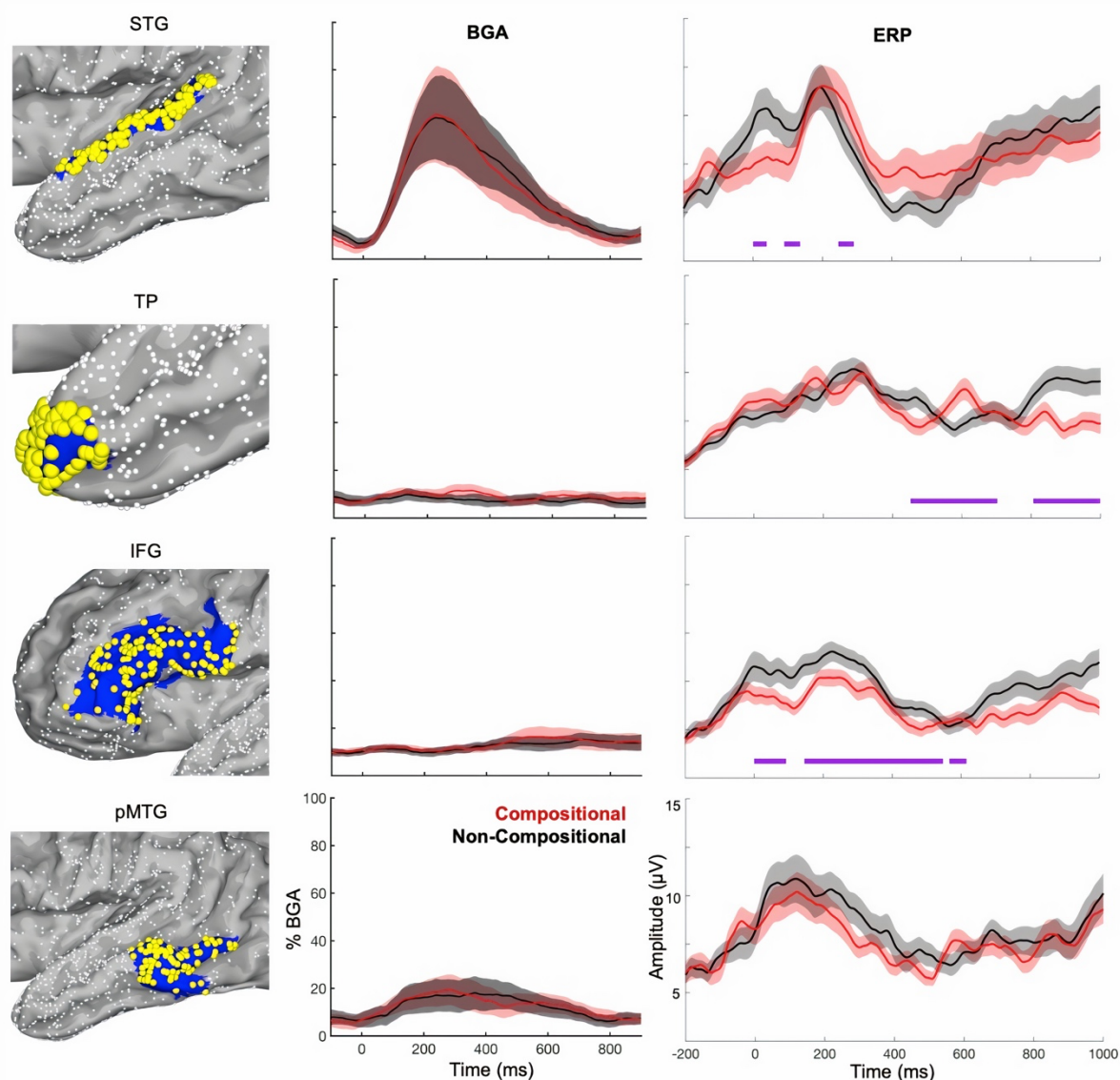


856

857 **Supplementary Figure 1: Inter-trial phase coherence and lexicity.**

858 (A) Electrodes with significant differences in ITC for words vs pseudowords, in a portion of
859 posterior temporal cortex with a high concentration of electrodes exhibiting significant
860 differences (9 patients); HCP index: area STV (Glasser et al., 2016). (B) Gamma traces (green
861 dashed box) for electrodes in (A) for words vs. pseudowords and compositional vs. non-
862 compositional trials (C) ITC in alpha (8-12Hz) for all electrodes in (A) for words (blue) and
863 pseudowords (red) on the left, with alpha (orange dashed box) amplitude traces, and for
864 phrase composition (purple) and non-composition (black) on the right isolated around the
865 onset of the second word (no significant effect for composition contrast). T0 = first word onset.

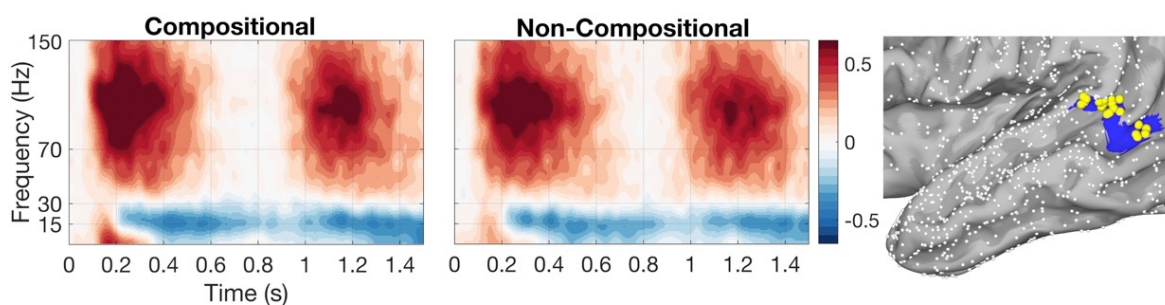
866



867

868 **Supplementary Figure 2: Regions of interest and their BGA/ERP signatures.** Regional
 869 broadband gamma amplitude (middle column) with event-related potentials (right column).
 870 Red: Compositional. Black: Non-Compositional. HCP index from top-down: posterior superior
 871 temporal gyrus (pSTG) = [A4]; temporal pole = [TGd]; inferior frontal gyrus (IFG) = [FOP4, 44,
 872 45, IFSp, p47r, IFSa, 47I]; posterior middle temporal gyrus (pMTG) = [PHT, TE1p]. BGA traces
 873 are thresholded by $p < 0.05$ significantly active from baseline (first word onset, -500 to -100ms)
 874 with a minimum of 10% BGA amplitude increase during the 100-400ms post-second word
 875 onset period. ERPs were computed across the four ROIs plotted on the left column, with
 876 significant condition differences being computed across 0-1000ms in the same (FDR-
 877 corrected) manner as the BGA plots (see Methods).

878

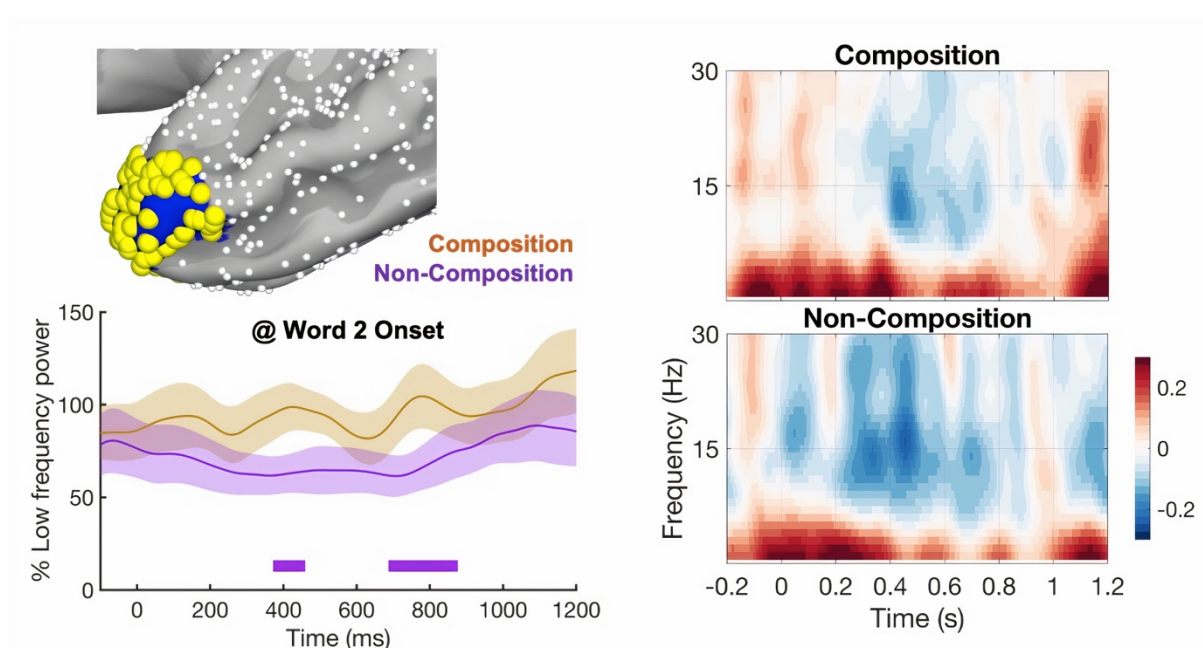


879

880 **Supplementary Figure 3: pSTS-TOJ regional spectrograms.** Spectrograms and electrodes

881 in pSTS-TOJ for all active channels (HCP index: TPOJ1; electrodes = 23, patients = 10).

882 Second word onset was at 800ms.



883

884 **Supplementary Figure 4: Temporal pole effects.** Low frequency (2–15Hz) temporal pole

885 trace with FDR-significant bars for the Compositional (brown) vs Non-Compositional (purple)

886 contrast (HCP index: TGd) with spectrograms, thresholded at 10% increased activity from

887 baseline; T0 = second word onset. For BGA, see Suppl. Fig. 2.